EFFECT OF ACCELERATION ON MATERIAL PROPERTIES

NOVEMBER 1972 — NUMBER 37

BY

HARI D. SHARMA

JHRP

JOINT HIGHWAY RESEARCH PROJECT

PURDUE UNIVERSITY AND
INDIANA STATE HIGHWAY COMMISSION

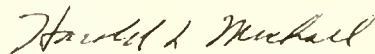Interim Report

EFFECT OF ACCELERATION ON MATERIAL PROPERTIES

TO: J. F. McLaughlin, Director   November 9, 1972
        Joint Highway Research Project
                                            Project: C-36-63E
FROM: H. L. Michael, Associate Director
        Joint Highway Research Project   File: 9-7-5

        The attached Report titled "Effect of Acceleration on
Material Properties" is an Interim Report on the HPR Part
II Research Study titled "Invariant Properties of Highway
Materials". Mr. Hari D. Sharma, Graduate Instructor in
Research, has authored this Report with the advice and
counsel of Professor M. E. Harr.

        The objective of this Study is to determine the effect
of accelerations on material properties and to develop
procedures for measuring these properties if the effect
cannot be ignored. The research reported herein indicates
that for the materials tested there is an effect on the
usually measured parameters if accelerations are involved.

        The Report is submitted for acceptance as partial
fulfillment of the objectives of this Study. It will be
submitted for review, comment and similar acceptance to the
ISHC and FHWA as it resulted from an HPR Study.

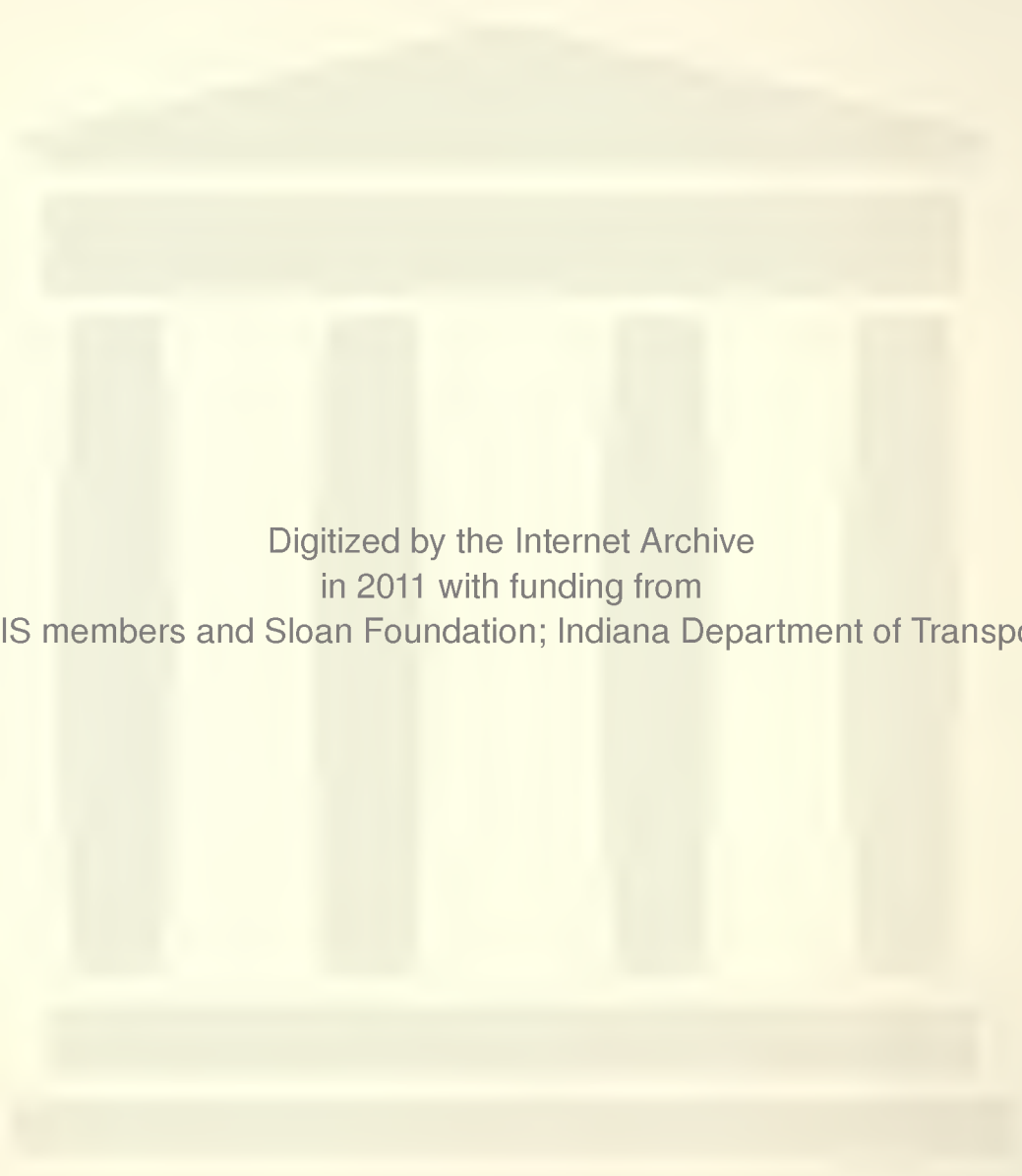   Respectfully submitted,

                        Harold L. Michael
                        Associate Director

HLM:ms

cc: W. L. Dolch   M. L. Hayes   C. F. Scholer
     R. L. Eskew   C. W. Lovell   M. B. Scott
     W. H. Goetz   G. W. Marks   J. A. Spooner
     M. J. Gutzwiller   R. D. Miles   N. W. Steinkamp
     G. K. Hallock   J. W. Miller   H. R. J. Walsh
     R. H. Harrell   G. T. Satterly   E. J. Yoder

Interim Report

EFFECT OF ACCELERATION ON MATERIAL PROPERTIES

by

Hari D. Sharma
Graduate Instructor in Research

ACKNOWLEDGMENTS

TABLE OF CONTENTS

TABLE OF CONTENTS, continued

LIST OF TABLES

LIST OF FIGURES

LIST OF FIGURES, continued

LIST OF FIGURES, continued

LIST OF SYMBOLS

A	area
a_x	acceleration in x direction
a_y	acceleration in y direction
a_z	acceleration in z direction
c	cohesion intercept
e_o	initial void ratio
e_{1g}	void ratio under static conditions (1g)
g	acceleration due to gravity
Ho	original thickness of sand layer
ΔH	settlement of sand layer
K	ratio of centrifugal force to the force of gravity
k	a constant
L	length
m	mass unit weight
n	number of revolutions per minute
p_i	inside pressure in the hollow cylinder
p_o	outside pressure in the hollow cylinder
q_u	unconfined compressive strength
r	radius of centrifuge
r_i	inside radius of hollow cylinder
r_o	outside radius of hollow cylinder

LIST OF SYMBOLS, continued

s   strength; arbitrary stress

T   temperature

u_a pressure in air

u_w pressure in water

u   displacement in x direction; pore pressure

V   velocity of rotation

v   displacement in y direction

w   displacement in z direction

α ratio of acceleration experienced by body while
            in centrifuge to that acceleration due to gravity

γ unit weight of material

Δ increment

ϵ strain

ρ mass unit weight

σ total stress

$\bar{\sigma}$ effective stress

σ_1 major principal stress

σ_2 intermediate principal stress

σ_3 minor principal stress

σ_a normal stress in axial direction

σ_c confining pressure

σ_r normal stress in radial direction

$\sigma_x, \sigma_y, \sigma_z$ normal stress in x,y,z directions, respectively

σ_θ normal stress in tangential direction

τ shear stress

τ_{ff} shear strength

LIST OF SYMBOLS, continued

τ_{xy} shear stress in x direction on a plane normal
          to y direction

τ_{yz} shear stress in y direction on a plane normal
          to z direction

τ_{zx} shear stress in z direction on a plane normal
          to x direction

ϕ friction angle

χ coefficient relating pore pressure in gas and
          water phases in soil

ψ constant

μ Poisson's ratio

ABSTRACT

Sharma, Hari D., Ph.D., Purdue University, December 1972.
Effect of Acceleration on Material Properties. Major
Professor: Milton E. Harr.

Theory indicates that, if accelerations are ignored,
the parameters c, ϕ, and γ are sufficient to characterize
a material with respect to its strength. However, these
parameters are insufficient for material strength character-
ization, if accelerations cannot be neglected. Any study
to determine significant and necessary basic properties of
materials must, therefore, include the determination of
the effect of accelerations on material properties.

The two-fold objective of this study is to determine
the effect of accelerations on material properties and to
develop procedures for measuring these properties.

A special centrifuge testing device has been designed,
constructed and calibrated for this study. In this device
accelerations can be changed at will. A VIDAR-5404-
Teletype writer with printed page and punched tape record
was employed as the data recording system.

Three materials were studied: an asphaltic mix (bound),
a cohesionless soil (unbound), and a cohesive soil (electro-
chemical bonding).

Triaxial compression tests on sheet-asphalt samples reveal that both strength parameters, c and ϕ, decrease as accelerations are increased (greater than lg). Parameters (c and ϕ) obtained from hollow cylinder tests are seen to be higher than the corresponding values obtained from the triaxial tests. A few tests were conducted on dry sand for comparisons. Then samples show that for a given confining pressure accelerations may decrease the void ratio. Triaxial compression tests on this dry cohesionless soil show a slight initial increase in shear strength with accelerations. A few unconfined compression tests were also conducted on a compacted cohesive soil. These indicate that the cohesion parameter, c, appears to decrease slightly as accelerations are increased (greater than lg).

INTRODUCTION

Although hard-won experience has wrought some modi-
fications in the planning of roads and airport runways, the
structural designs for building them are much the same as
those used in yesteryear's carriage ways. This assumes
that the loading is static - that the only thing that
counts is the dead weight of the vehicle. Yet once a
plane, truck, or car starts moving, its motion sets up
a very different situation in the pavement.

If one considers a point in a pavement ahead of a vehi-
cle, the point begins to move even before the vehicle gets
there, responding to the energy wave generated by the
vehicle. Generally the point ahead will first be subjected
to compressive loadings. Then, with the passage of the
vehicle, there will be tensile stress. Certainly, this is
no static problem. Moreover, secondary waves and surface
waves will be generated in the vicinity of the vehicle.
Thus, considerable energy is transmitted in all
directions from a vehicle moving on a pavement. This energy
produces accelerations and the loading on the pavement
element becomes of dynamic nature.

In spite of the dynamic loadings and induced acceler-
ations experienced by pavements during their lifetime, all
existing methods of pavement design and all coexistent
laboratory tests are predicted on static considerations
only. At best, the passage of a stream of traffic is
accomodated as an "equivalent" number of static load repe-
titions. Thus it is not surprising that only minimal
success has been achieved in the prediction of field
behavior of pavements.

Since the first highway, engineers have sought those
characteristics of material that would reflect their action
under field loadings. Developing concurrently with the
strength of materials philosophy (in the early 1900's),
they were primarily concerned with qualitative determina-
tions that would indicate whether materials met minimum
standards. These tests developed rapidly and today provide
the bulk of the laboratory procedures used in highway work.

All laboratory tests simply quantify some preconceived
theory. Therefore, first the underlying theoretical frame-
work customarily involved for stability investigations
into the structural adequacy of materials will be restated.
Following this, attention will be directed to the more
realistic development of the current work and of centri-
fuge testing in which accelerations can be changed at will.

BACKGROUND AND SIGNIFICANCE OF WORK

Accepting the concept that stress is a measure of the transfer of forces through a body, at any point within a body, the equations of motion are (Harr, 1966):

$$\frac{\partial \sigma_x}{\partial x} + \frac{\partial \tau_{xy}}{\partial y} + \frac{\partial \tau_{xz}}{\partial z} = \rho \frac{\partial^2 u}{\partial t^2} = \rho a_x$$

$$\frac{\partial \tau_{xy}}{\partial x} + \frac{\partial \sigma_y}{\partial y} + \frac{\partial \tau_{yz}}{\partial z} = \rho \frac{\partial^2 v}{\partial t^2} = \rho a_y \tag{1}$$

$$\frac{\partial \tau_{xz}}{\partial x} + \frac{\partial \tau_{yz}}{\partial y} + \frac{\partial \sigma_z}{\partial z} - \gamma = \rho \frac{\partial^2 w}{\partial t^2} = \rho a_z$$

where σ denotes the normal stress, τ the shear stress and u,v,w are the displacements, and a_x, a_y, a_z the accelerations in the x,y,z directions, respectively. γ is the unit weight of the material under consideration, and ρ is the mass unit weight ($\rho = \gamma/g$). These expressions are valid irrespective of material, they require only the validity of Newton's second law of motion (F = ma). As these expressions contain 9 unknowns (3 unknown normal stresses, 3 unknown shearing stresses, and 3 unknown displacements) in 3 equations, the resulting system is seen to be

indeterminate. That is, at least 6 more independent expres-
sions relating these unknowns are needed to render the
system solvable.

To achieve a balance between unknowns and equations
for the system in Eqns. (1), recourse must be made to further
assumptions. Generally, these assumptions are predicted
less on the observed action of materials to load than on
whether the resulting equations can be solved in the
mathematical sense. For example, in the classical theory
of elasticity, recourse is made to the definition of the
geometric theory of strain and the assumption of a linear
and homogeneous relationship between the strains and stress-
es (Hooke's law). In addition, after pleading isotropy
which reduces the 36 parameters (elastic properties) to 2,
the developed parameters (E and μ) are also taken to be
independent of time and to extend their validity to collec-
tions of points, or to bodies. In theories of plasticity
and viscoelasticity similar relations are instituted in
terms of rates or expressions are introduced at limiting
conditions.

At limiting equilibrium (an assumption that restricts
consideration to equilibrium conditions to being, hypo-
thetically just at the verge of failure), the right hand
terms of Eqns. (1), ρa_x, ρa_y, ρa_z, vanish and the imbalance
reduces to 6 unknowns in 3 equations. Pleading geometrical
license, further simplifications follow upon   the

introduction of a "condition" of plane strain or upon
simply ignoring the existence of one of the three spatial
dimensions. Either assumption when combined with that
of limiting equilibrium will then render the three equa-
tions (1) to the two expressions

$$\frac{\partial \sigma_x}{\partial x} + \frac{\partial \tau_{xz}}{\partial z} = 0$$

$$\frac{\partial \tau_{xz}}{\partial x} + \frac{\partial \sigma_z}{\partial z} = \gamma$$

(2)

Expressions (2) indicate that the system is now re-
duced to three unknowns in two equations. Should another
independent expression exist that could relate the three
stresses in a unique way, the resulting system would then
be statically determinate. The third equation is generally
provided by the Mohr-Coulomb "strength" relationship,

$$\sin^2\phi(\sigma_x + \sigma_z + 2 c \cot \phi)^2 = (\sigma_x - \sigma_z)^2 + 4\tau_{xz}^2$$

(3)

which, in turn, contains the two "strength" parameters; c
and ϕ. Equations (2) and (3) provide the bulk of the
theoretical framework for stability investigations into
the structural adequacy of aggregate materials (e.g. soils
and asphalt mixes).

To render Eqns. (2) and (3) in non-dimensional form,
the following dimensionless variables are defined

$$x' = \frac{x}{L}, \quad z' = \frac{z}{L}, \quad \sigma'_x = \frac{\sigma_x}{s}, \quad \sigma'_z = \frac{\sigma_z}{s},$$

$$\tau'_{xz} = \frac{\tau_{xz}}{s} \tag{4}$$

where L and s are an arbitrary length and an arbitrary
stress, respectively. Substitution of these expressions
into Eqns. (2) and (3) yields

$$\frac{\partial \sigma'_x}{\partial x'} + \frac{\partial \tau'_{xz}}{\partial z'} = 0, \quad \frac{\partial \tau'_{xz}}{\partial x'} + \frac{\partial \sigma'_z}{\partial z'} = \frac{\gamma L}{s}$$

$$\sin^2\phi\left(\sigma'_x + \sigma'_z + 2\,\frac{c}{s}\cot\phi\right)^2 = (\sigma'_x - \sigma'_z)^2 + 4\tau'^2_{xz} \tag{5}$$

Eqns. (5) demonstrate that, in general, Eqns.
(2) and (3) do not satisfy similitude. This
means that geometrically similar regions will not neces-
sarily yield similar results. Thus, if c and ϕ are
determined from a test of given dimensions, it should not
be expected that the same numerical values would follow
if the dimensions were changed; even though the ratio of
their dimensions were held constant. Also, the third
expression is seen to be non-linear and hence indicates
(as is true for "bearing capacity") that superposition is
not generally valid. Furthermore, Eqns. (5) demonstrate
that the so-called "strength parameters" c and ϕ might be
expected to be influenced to a considerable degree by
changes in the density of the material.

The foregoing demonstrated several presuppositions into the approach of assessing the adequacy of materials. To summarize: it was assumed that (a) plane strain prevailed, (b) the system was in equilibrium, (c) point-wise attributes could be extended to bodies, and (d) the density of the materials was an invariant with time. The two parameters c and ϕ were isolated after invoking the above postulates.* Should field conditions exist which do not deviate greatly from these, it might be expected that the two parameters would serve well to designate the adequacies of designs. In particular an element in a highway, during the passage of a vehicle, is not generally in plane strain, and displays considerable changes in velocity and in volume with time. Hence, it should not be expected that these two parameters alone will be adequate to the task. This thesis addresses the questions of what additional properties might be needed, their effect and how their measure might be obtained.

As previously noted, Equations (2 and 3) indicated that if accelerations are ignored, the parameters c and ϕ and γ were sufficient to characterize a material as a balance was achieved between equations and unknowns. If the accelerations can not be neglected, they would take the form:

---

* Although in conventional testing c and ϕ are sometimes evaluated when density changes with time during shearing.

$$\frac{\partial \sigma_x}{\partial x} + \frac{\partial \tau_{xz}}{\partial z} = \rho \frac{\partial^2 u}{\partial t^2}$$

$$\frac{\partial \tau_{xz}}{\partial x} + \frac{\partial \sigma_z}{\partial z} = \gamma + \rho \frac{\partial^2 w}{\partial t^2}$$

(6)

Whereas the 2 expressions contain 5 unknowns, one additional equation, such as Eqn. (3) can not provide a unique system: 2 additional independent expressions are required. As was found to be the case for Eqn. (3), the physics of the system suggests that each of the necessary two expressions will contain at least one new parameter. Whereas the need for these expressions come about from the introduction of the inertia terms, it might be expected that the parameters will be acceleration dependent.

Ideally, to permit a quantitative evaluation of the adequacy of a component material in a structure, what is sought is a simple laboratory procedure which yields numbers that will reflect the material's response under field conditions. Should such numbers exist they would be true _properties_ of the materials. Whereas such parameters are required to remain unchanged while bridging the gap between laboratory and field conditions, they can be said to be _invariants_. Methods of design and prediction of performance become highly reliable when the material invariants are available.

The twofold objectives of this research are, there-
fore, to determine significant and necessary basic proper-
ties of materials and to develop laboratory procedures
for measuring these properties.

REVIEW OF LITERATURE

Development of Technique for Variation of
Gravitational (Acceleration) Fields

This review of literature is concerned mainly with gravity variational techniques which have been used in the past by various investigators. The techniques are 1) by Centrifuge Method and 2) by Maneuvers of Aircraft. In all of these studies where centrifuge was used as a tool, it was used either to take into account the body forces or to study model-prototype relationships. The literature indicates that no tests have been conducted, employing a centrifuge, to determine the effects of accelerations on strength and volume change properties of materials.

Centrifuge Method

Bucky (1931) discussed the use of centrifugal models in the study of mining structures. Author's comments on the principle of centrifuge testing follows:

> If in the model, the pull of gravity of each part can be increased in the same proportion as the linear scale is decreased, then the unit stress at similar points in the model and proto-type will be the same, and the displacement or deflection of any point in the model will

represent to scale the displacement of the corresponding point in the prototype.

In this paper of Bucky (1931), two experiments were described that verified the theory by testing small rectangular beams of various materials.

Bucky et al (1935) described the centrifugal method of testing combined with the photoelastic method of stress measurement. This combined method opened a new field which led to the study of heavy structures by modeling.

Pokrovsky and Fedorov (1936) studied soil problems by means of modeling with the aid of centrifuge. The problems studied were the stability of slopes in earth banks and in cuts and the distribution of pressures under foundations. Results of model and theory were compared with field measurements. Similar apparatus was used for determination of pressure on culvert pipes. Model and field experimental results were also compared for foundation settlements. The two test results were found to be in close agreement.

Panke (1952) investigated structures in which strains of significant magnitude are produced by their own weight. This was thought to be applicable to the design of mine openings and to the study of some ground-control problems.

In the previous applications of centrifugal testing by other investigators (Bucky 1931, Bucky et al 1935) the models usually were tested to failure, and the

analysis was made from the type of break produced. The
models were tested of the same materials as the proto-
type, and the test results were applied only to particu-
lar prototype represented by the model. Deflections
were measured from the photographs of the rotating model,
but no means was employed either to determine the actual
distribution of stress in the model or to determine
quantitatively the degree of restraint imposed on the
ends of the loaded model beam, i.e., to determine whether
the loaded model behaves as a beam with rigidly fixed
ends or as some other type of beam.

The centrifugal-testing apparatus designed by Panke
(1952) was unique in that it incorporated the use of
resistance gages to measure directly the strains in a
rotating model without testing it to failure. The
apparatus had a design radius of rotation of 2 ft. with
a maximum speed of rotation of 2,000 r.p.m.. With this
apparatus it was possible to determine the state of strain,
and thus boundary conditions, in a rotating model weigh-
ing up to 90 lbs. A model, in this apparatus, could be
subjected to a centrifugal force up to about 2,600 times
the force of gravity.

Rambosek (1964) conducted experiments by loading a
two-dimensional photoelastic model which simulated a thin
slice through an open pit. This was not possible by the
application of uniaxial load, because it did not simulate

the effects of increasing depth of overburden. Body-loading a transparent urethane rubber model by centrifuging was selected as the technique by which "gravitational" effects could be best simulated. By this method "surface" loads were zero, and stresses in the model increased as the "depth" below surface increased.

This report described a four-foot radius centrifuge, designed so that the stress patterns could be observed or photographically recorded as a transparent, two dimensional photoelastic model is body-loaded by centrifuging at any desired speed up to an effective maximum of 250 rpm. The centrifuge pit was of reinforced concrete construction, having an inside radius of 49 inch and depth 60 inch. Accessory components consisted of polarizing elements, a suitable high intensity, externally triggered stroboscopic light source, recording equipment and other necessary controls were used.

Avgherinos and Schofield (1969) conducted investigations to develop a better understanding of the drawdown failures of centrifuged models. In summarizing their work, the authors state:

> In the model tests using natural soil correct modelling of both compression and yielding may be achieved in centrifugal test facility when the acceleration is increased by the same factor by which the model scale is reduced. Compression and yielding of soil phase and transient flow of pore fluid phase will occur simultaneously and transient flow is then correctly modelled with the usual reduction of time scale by the square of the

model scale factor. To develop this technique plane section models of cuttings were tested. Saturated kaolin clay was consolidated from twice the liquid limit into block specimens. The blocks were trimmed as cutting section models, placed in a strong box on a centrifuge, accelerated and flooded with water. External operation of a valve and drainage of water produced sudden draw-down. Failure of the cutting slope was observed visually with stroboscopic illumination and flash photography.

Mikasa et al (1969) developed a centrifugal apparatus to test the stability of model slopes under the same stress conditions as the prototype. The model container could be put in a centrifugal acceleration field of 200g, and could be inclined through ± 16.7 degrees during rotation. Kisen-Yama Rockfill Dam, 90 meter in height, was examined by this apparatus both for earthquake and for rapid drawdown conditions. The test results were then compared with the result of conventional stability calculation. Among Mikasa's conclusions is the following:

The centrifugal test method was proved to be useful for investigating the failure conditions of slopes, and for getting the relations between the strength parameters from the shear test and the strength of a soil mass under the stress condition similar to the prototype dam.

Lyndon and Schofield (1970) reported the extension of Avgherinos and Schofields centrifuge model test results. These tests were performed in order to study the short-term stability of excavations in stiff fissured London clay. No definite conclusion was drawn from these tests.

The Maneuvers of Aircraft

Johnson et al (1969) worked with a different tech-
nique of gravity variation by flying the test container
in an aircraft through carefully controlled maneuvers to
simulate 0.17, 0.38, and 2.5 times terrestrial gravity.
An experimental investigation was conducted to determine
the effects of varying gravity and atmospheric pressure
on the size of small explosion craters formed in cohesion-
less sand. It was concluded that both gravity and
atmospheric pressure, when varied, will lead to signifi-
cant changes in crater dimensions. The ratio of crater
diameters was inversely proporational to the ratio of
gravities to the power n, where n increased as the depth
of burst of the explosive increases. In other words,
if mobilized strength was assumed to be some function
of crater diameter then it could be concluded that strength
increased with acceleration fields.

Field Accelerations

At the present time there exists no reliable measure-
ments of the accelerations a highway pavement experiences
during the passage of a vehicle. Recent tests conducted
at Kirtland Air Force Base (Boyer, 1972) on runways indi-
cated pavement accelerations may be as high as 2.9g.
Some information is also available in the literature for
some other structures.

It has been observed that earthquakes may cause vertical accelerations of the surface of the ground on the order of 1.3g (Lambe and Whitman, 1969; Seed and Idriss, 1971). Recorded accelerations of soil close to hammer foundations have values of the order of 1.7 to 2.0g (Barkan, 1960). Some tests conducted by NASA (Lee and Scheffel, 1968) on runways indicate cockpit acceleration may be on the order of 1.4g. Accelerations up to 1.67g were measured in tire pressures during the AASHO Road Test (HRB Special Report 6) under normal conditions and 2.4g maximum when the vehicle dropped from a prepared ramp. Recognizing that inherently greater roughness may exist in highway pavements than airfield runways because of the greater number of joints and the greater curling and warping of these pavements, it is not unreasonable to expect that relatively high accelerations may exist on highway pavements, at critical times, upon the passage of a multi-wheeled truck.

Hollow Cylinder Test Techniques and
Their Development

Hollow cylinder test, unlike the conventional solid cylinder test is truly triaxial in nature. On one hand it provides the means of providing variations in the three principal stresses on the other it provides a closer definition of stress because its area of cross section

being small. Details of hollow cylinder tests are re-
viewed because it is a comparatively new technique in
material testing methods.

Kirkpatrick (1957) performed the hollow cylinder
tests on sand. The test was conducted by first setting
the outside fluid pressure and then slowly increasing the
inside fluid pressure until failure occurred. The axial
stresses were calculated by knowing the outside and in-
side pressures at failure. The analysis of his test
results demonstrated the yield surface to be the hexagonal
pyramid being consistent with the Mohr-Coulomb criterion.
Based on the comparison of hollow and solid cylinder
testings Kirkpatrick also indicated that hollow cylinders
produced slightly greater ϕ value than the solid cylinder.

Whitman and Luscher (1962) conducted tests with the
hollow-cylinder device similar to Kirkpatrick. They
verified experimentally the case when failure is brought
about by increasing the outside pressure. Back-calculat-
ing from test results with different sand densities and
sample geometry they found the plot of the calculated ϕ
values versus pressure ratios to fall on the same
straight line. ϕ values obtained from hollow cylinders
were found to exceed the values from solid cylinder test-
ing verifying the previous investigation (Kirkpatrick,
1957).

Wu, Loh and Malvern (1963) also presented the experimental study of Mohr-Coulomb failure criterion in three-dimensional stress space. In this investigation hollow cylinder tests were conducted and all the three principal stresses were varied independently. Both sand and clay were used in the tests. In addition to this the conventional triaxial (solid cylinder) compression and extension tests were also performed on cylindrical specimens of remolded clay and sand. The experimental results on clay agreed well with the Mohr-Coulomb failure envelope expressed in terms of the Hvorslev strength parameters. It was concluded that the undrained strength of clay was independent of the intermediate principal stress and of stress path during loading. The strength of sand was found to be dependent on the intermediate principal stress.

Objective of Study

From the brief review presented it appears that no successful attempt was ever made to make use of these available acceleration variational techniques for the determination of basic strength properties of materials. It is the objective of this study to develop such a testing technique for general highway materials, and to determine necessary basic properties of these materials.

CENTRIFUGE TESTING

General

A gravitational force equal to mg, directed normal to the earth surface, acts on all bodies at the surface, where m is the mass of the body and g is approximately 32.2 ft/$\sec^2$. When a body is placed in a centrifuge and rotated an additional force is generated equal to mV^2/r, where V is the velocity of rotation and r the radius of the path. The centrifugal force acts in the radial direction, away from the center of rotation. The ratio K of the centrifugal force to the force of gravity is

$$K = \frac{V^2}{gr} = \frac{4\pi^2 rn^2}{g} \tag{7}$$

where n is the number of revolutions per minute. The ratio of acceleration experienced by the body while in the centrifuge to that due to gravity alone, Fig. 1, is

$$\alpha = \sqrt{1 + K^2} \tag{8}$$
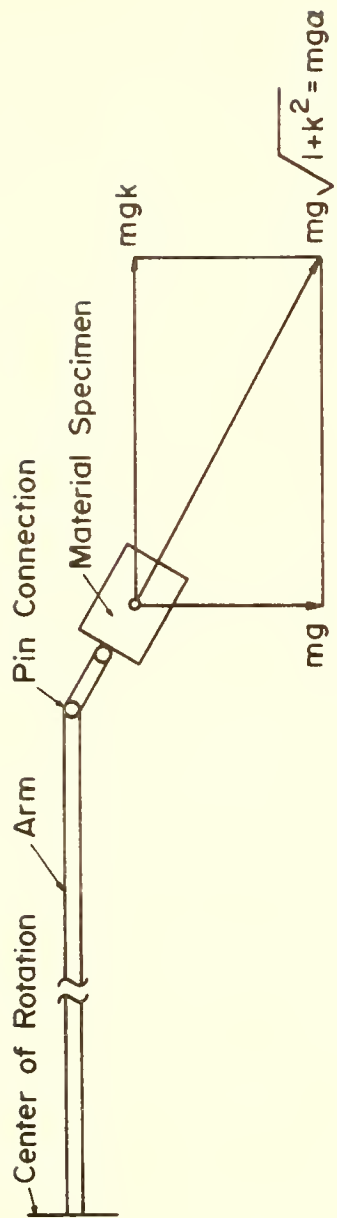
FIGURE 1   SPECIMEN HANGING IN RESULTANT ACCELERATION FIELD .

Apparatus

A centrifuge testing device was constructed as shown
schematically in Figs. 2 and 3. The material specimen
container is attached at one end of the arm and balancing
counter weights at the other. The arm rotates in hori-
zontal plane. The container and the counterweights are
pinned to the arm and hence hang in the direction of the
resultant of the gravity and centrifugal forces, Fig. 1.
Some specifications of this apparatus are summarized in
Table 1.

Table 1. Specifications of Apparatus

Specimen container	Cylindrical hollow aluminum cylinder 5 inches high and 3-1/2 inches internal diameter (details are shown in Fig. 4)
Radius of rotation	41.00 inches (to the mid-height of the container)
Rate of rotation	300 rpm, max.
Centrifugal acceleration	Maximum $\alpha g = 104$ g (where "g" is the acceleration of gravity)
Motor for centrifuge rotation	1672 KW, 1720 RPM
Motor to drive lead screw	27 V, DC, 250 RPM

The centrifuge was powered by a 2 horsepower electric
motor using a V-belt and pulley drive. The speed of the
motor and the rotation of the centrifuge arm was controlled

22

Counter Weight

Smaller Gas Cylinder

Pressure from Larger Gas Cylinder

Rotary Joint

Specimen Container and Loading Set Up

Slip Rings

Motor to Drive Centrifuge
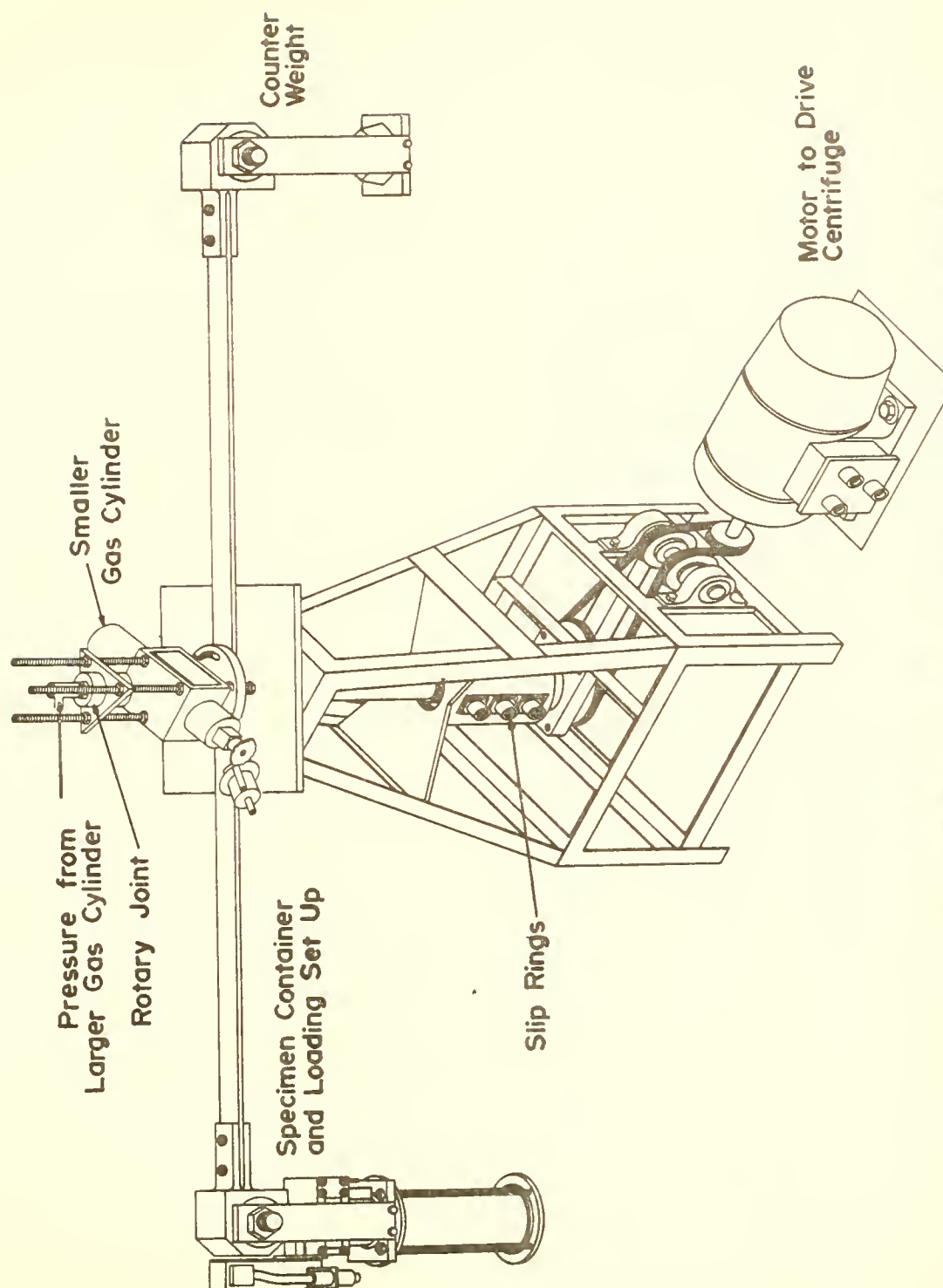
FIGURE 2 SCHEMATIC VIEW OF THE CENTRIFUGE SET UP

Displacement Potentiometer

Motor to Drive
Lead Screw

Worm Gear

Load Cell

Specimen Container
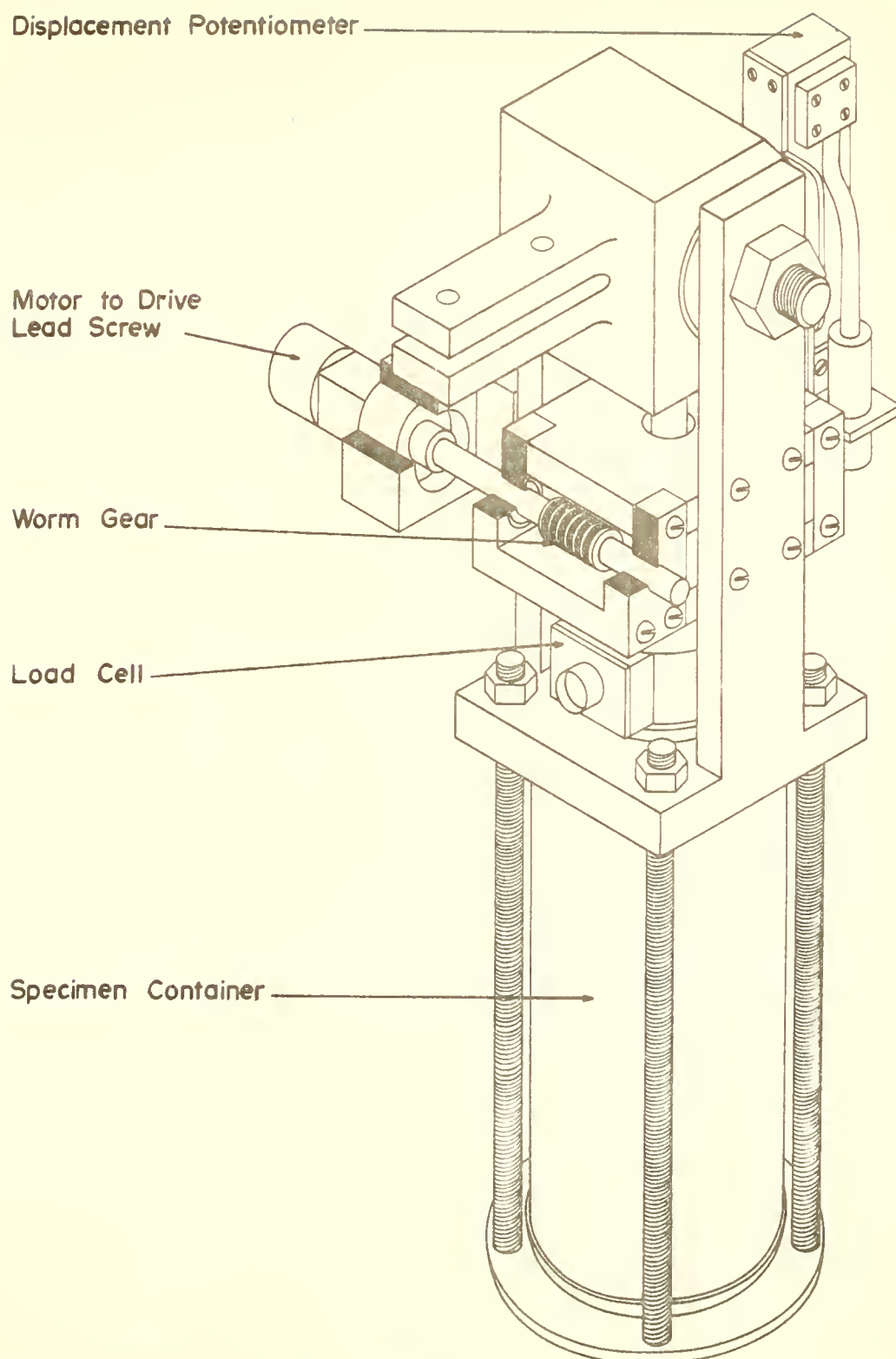
FIGURE 3 DETAILS OF LOADING ASSEMBLY.

FIGURE 4   DETAILS OF SPECIMEN CONTAINER.

by a transformer. The speed of rotation was obtained
through a cam operated switch.

Confining pressure application arrangement consisted
of two gas tanks. One tank (the smaller of the two) was
attached at the top of central plate above rotating arms.
The second cylinder (the bigger of the two) was connected
to the centrifuge through a rotary joint (Fig. 2). In
triaxial testing only the second gas tank was used for
applying confining pressures to material specimen. Both
tanks were utilized in hollow cylinder tests: the in-
ternal pressure was applied by the bigger gas tank and
external pressure by the smaller one.

An axial load could be applied to the specimen through
a 300 lbs. capacity load cell containing a four-arm bonded
strain gage bridge, with all connections made at the
minimum stress points. The compression of the sample was
monitored by a linear displacement potentiometer, whose
end points are at 10 volts potential difference.

Load application on the specimen was achieved by
strain control through the use of a lead screw and worm
gear assembly driven by a 27 volts DC motor. The specimen
is housed inside an aluminum cylindrical shell, which is
in turn fixed to a pin (Figs. 5 and 6) of the arm so as
to hang freely in the direction of the resultant of
gravity and the centrifugal force.

FIGURE 5 CENTRIFUGE SET UP.

FIGURE 6 DETAILS OF LOADING ASSEMBLY.

All signals from the rotating parts were taken out
through the slip rings. These are self-contained units,
in which the brush assembly is supported by shielded ball
bearings on a hollow-slip ring shaft. The entire assembly
slides over the shaft of the test device and is held in
place with locking screws. The leads were run through
the vertical hollow shaft of the test device.

VIDAR-5404-Teletypewriter with printed page and
punched tape record provided the data recording system
(Fig. 7). The integrating digital voltmeter measures
DC voltage. This signal is measured by converting it to
a frequency and counting the frequency for a known period
of time. Thus the counter provided the integral of input
voltage. The integration period is 100 m sec. Following
an external commands it can make up to 9 readings per
second. Without external commands it displays control
limits speed to 2 readings per second.

Materials Used in the Study

It was the objective of this research to investigate
a wide range of materials: asphaltic mixes (bound),
cohesionless soils (unbound), and cohesive soils (electro-
chemical bonding). Therefore, three series of tests were
conducted each using different material.

FIGURE   7   RECORDING AND CONTROL DEVICES.

Asphaltic Mix

A sheet-asphalt mixture was used for the first series of tests performed in this study. The test properties of the asphalt cement and aggregates used in the mixture are given below.

The asphalt cement used was of ASTM penetration grade 60-70. Standard ASTM tests indicated a penetration (100 gms., 5 sec. at 77°F) of 64 and a specific gravity at 77°F of 1.024. The asphalt content used in the mixture was 9.0 percent by weight of aggregate as was found previously to be optimum by Wood (1956).

The aggregate used was a natural material obtained locally. The sieve analysis of the chosen gradation is given in Table 2.

Table 2. Gradation of Aggregates

Passing	Retained	Grading
No. 8	No. 16	9
No. 16	No. 30	17
No. 30	No. 50	17
No. 50	No. 100	25
No. 100	No. 200	16
No. 200	Pan	16

e_{max} = 0.76, G_s = 2.64

e_{min} = 0.24, well graded sand (SW).

Cohesionless Soil

The second series of tests were conducted on a cohesionless soil. Grain size analysis of this cohesionless soil is given in Table 2. The soil used in the tests was oven dried.

Cohesive Soil

A third series of tests involved the laboratory compacted cohesive soil. The soil is a commercially available clay called grundite. The <u>clay</u> was an inorganic clay of high plasticity (CH) and had the following characteristics:

> Particle Size - 63% less than 2μ
> Liquid Limit (L.L.) = 52%
> Plastic Limit (P.L.) = 30%
> Specific Gravity (Gs) = 2.79
> Proctor standard optimum moisture
>   content (O.M.C.) = 21.5%

<u>Specimen Preparation</u>

Sand-Asphalt Samples

Cylindrical specimens, 1 inch in diameter and 2 inches high were fabricated and tested. A split mold was oiled inside with a very thin film of lubricating oil and assembled. The assembled mold together with a cylindrical plunger, mixing bowl, mixing spoon and tamping rod were placed in an oven at a temperature of 300°F. The mold and assembly are shown in Fig. 8. The different fractions

FIGURE 8   MOLD ASSEMBLY FOR SHEET-ASPHALT
SAMPLES.

of the aggregate were proportioned as was the calculated
quantity of 60-70 penetration asphalt cement. After pre-
heating both aggregate and asphalt to 300°F for 1 hour,
the specimen was placed in the split mold in three layers
and each layer tamped 30 blows. When rodding was complete
the plunger was fitted into the mold and this assembly
was then placed in a hydraulic compaction device. A
load was applied gradually until the compacted length
of specimen reached 2.25 inches. The mold was then turned
upside down and the procedure repeated to reach a specimen
of 2 inches height.

The hollow cylindrical specimens, 3 inches high
having 1.5-inch external and 0.5-inch internal diameters,
were made of the same composition of sheet asphalt and
were compacted to the same density as the solid cylindri-
cal test specimens. The procedure for the preparation
of these specimens was the same as that for solid cylindri-
cal specimens with the following modifications. The base
plate for the mold was fitted with a steel rod 0.5-inch
in diameter and 4 1/2 inches long. A 0.5-inch diameter
hole was provided in the center of the plunger to receive
the steel rod of the base plate. The mold and assembly
are shown in Fig. 9. After compaction, the specimen was
left resting on the base plate with the 0.5-inch diameter
rod passing through it. After the specimen had cooled,
the plunger was removed.

FIGURE 9 MOLD ASSEMBLY FOR HOLLOW CYLINDRICAL
SHEET ASPHALT SAMPLES.

Sand Samples

Cylindrical sand samples, 1 1/2 inch in diameter and 3 inches high were prepared for triaxial compression tests. A rubber membrane was first placed inside a split mold assembly. Then a predetermined weight of dry sand was compacted in this mold. The sand was placed in three layers and each layer tamped 25 blows. After the sample had been levelled, capped and sealed, suction (-0.35 kg/cm^2) was applied to give the sample sufficient strength to stand while the dimensions were measured and the cell assembled in the centrifuge device. The specimen and the assembly are shown in Figure 10.

Compacted Clay Samples

About 3000 grams of grundite were mixed with the required amount of water (to produce a water content of 21%) for about 30 minutes in the "Liquid-Solids twin shell blender" supplied by the Patterson-Kelley company. The mixed soil was stored for two weeks in an air-tight container to permit an equilibrium water content distribution.

A compaction mold having a 1-inch inside diameter and a 2-inch height, and six extension pieces was used to prepare the sample (Fig. 11). The extension pieces permitted compaction in six stages, by alternatively compacting both top and bottom, until the required height

FIGURE 10 ASSEMBLY FOR CYLINDRICAL SAND SAMPLES.

FIGURE II   COMPACTION MOLD FOR CLAY SAMPLES .

of 2 inches was reached. The heights of the extension pieces were 1/16", 1/8", 3/16", 1/4", 3/8" and 1". Two extension pieces were used at each stage, one at the top of the mold and the other at the bottom. The net amount of compaction done was the difference in thickness of the extension pieces. Similar method of compaction was used by Sridharan (1968).

A hydraulically controlled loading device was used to compact the sample statically. Static compaction method was selected because it yields the most uniform specimens (Gau and Olson, 1971). As the load was released, an elastic rebound of approximately 1/32-inch occurred at the top and bottom of the sample; this was trimmed away carefully with a very fine straight edge. This trimming also removed the highly stressed portion of the sample at the top and bottom ends. The sample was then extruded carefully from the mold, wrapped in polyethylene bags and sealed by dipped into the wax. The sealed sample was then stored in a humid chamber before testing. The molded unit weight of compacted samples was 2.14 gm/cm^3.

Testing Procedure

First, the field loading conditions will be discussed. Following this attention will be directed to laboratory testing procedures.

Field Loading

Vehicles traversing a pavement impart energy to it in a complicated manner. Consider three elements in a pavement system at the same transverse location, designated E_i (i = 1, 2, 3) in Figure 12 corresponding to the action of vehicles moving in the longitudinal direction (three positions P_j, j=1, 2, 3 are shown in the figure 12. Each vehicle position will produce very much different acceleration fields in the vicinity of the elements, depending upon their relative positions. For example, for element E_2, with the vehicle at position P_1, the resulting acceleration vector is primarily oriented in the positive X-direction. When directly over E_2 (not shown) the acceleration of E_2 would most likely be primarily vertical. The action of the element at E_2 with the vehicle at position P_3 depends not only on the energy transmitted to it directly from the vehicle at that position but also that previously inherited. For a vehicle at position P_2, the water becomes even more muddy.

Figure 13 shows an acceleration-time record of a point on an airport pavement during the passage of a Boeing 727 (Boyer, 1972). The plane was moving at approximately 25 mph. An accelerometer was palced 2.5 ft. from the center of the gear track. It is noted that the point was first subjected to compressive loading (along a-b). Then, with the passage of the vehicle, tensile stresses were observed
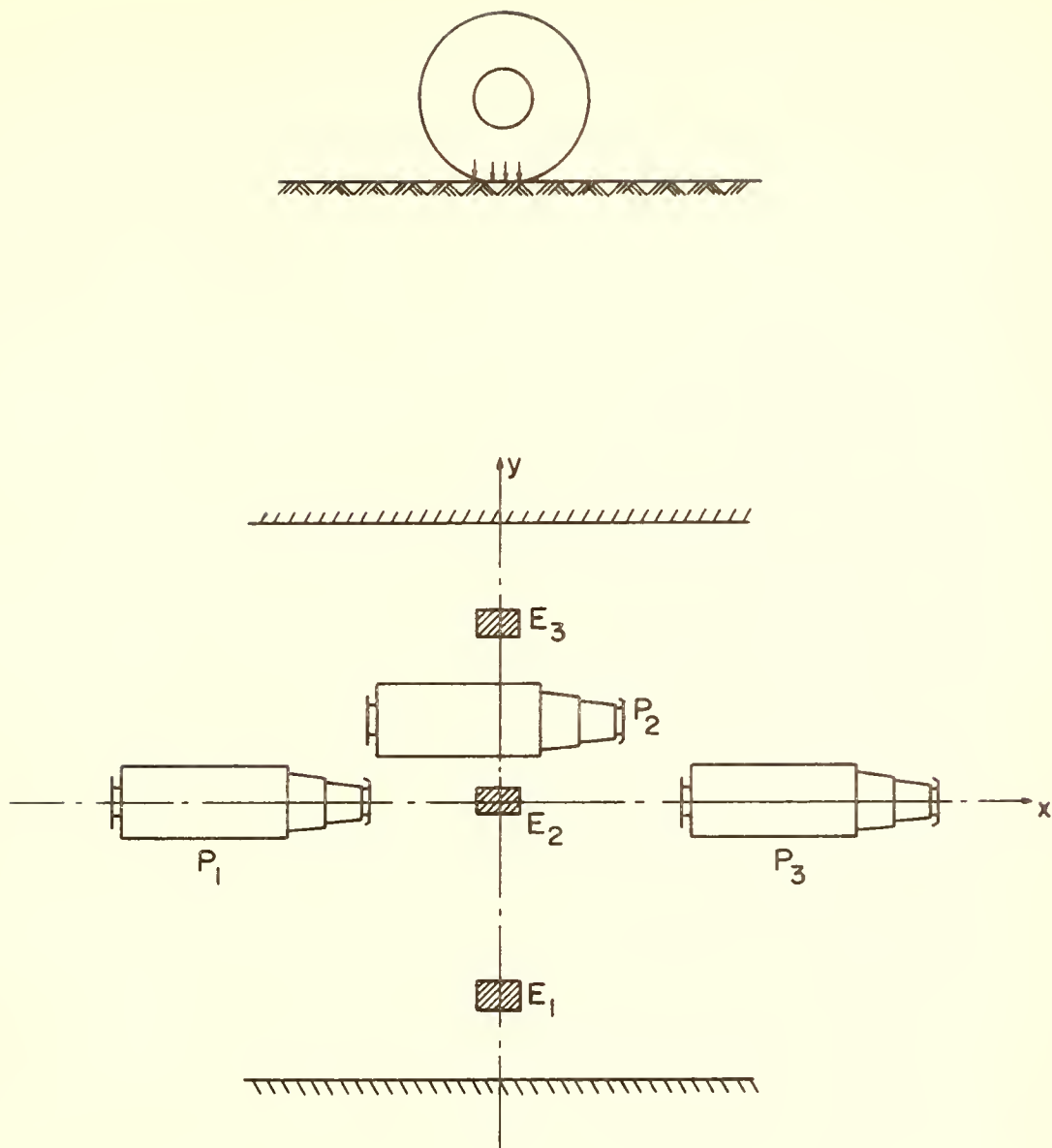
FIGURE 12   DIFFERENT VEHICLE POSITIONS IMPARTING
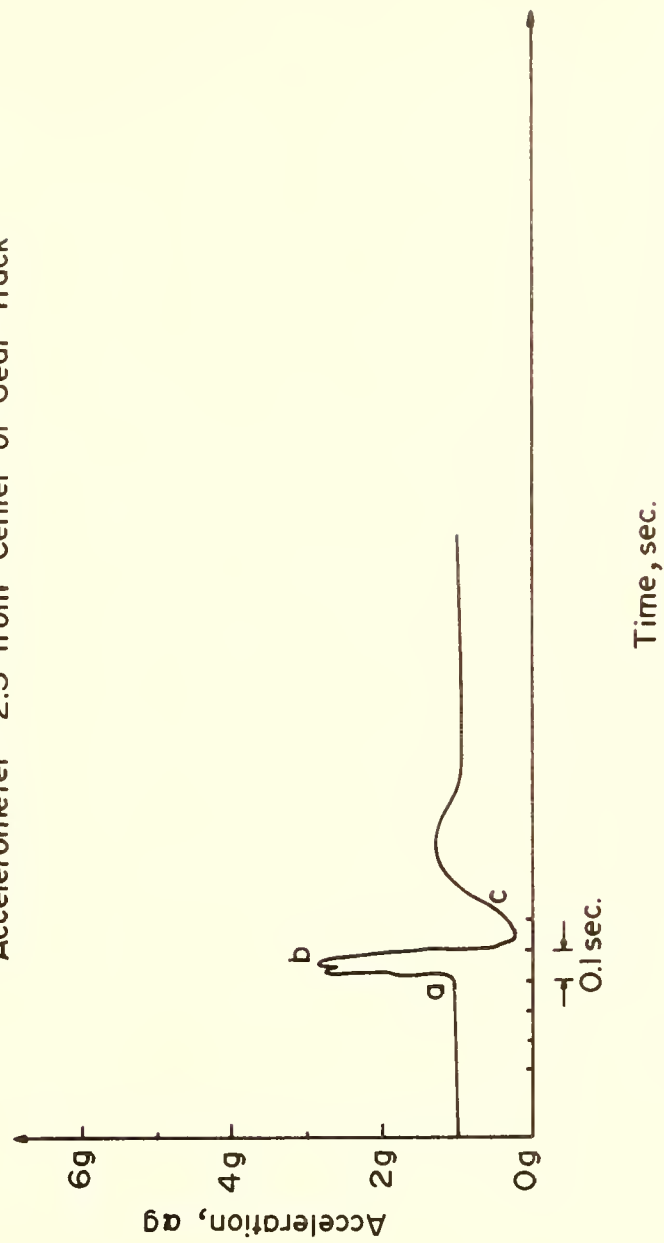ENERGY TO PAVEMENT.

FIGURE 13 ACCELERATION-TIME RECORD ON PAVEMENT FOR BOEING-727

(along b-c). It is believed a similar pattern of accelera-
tion would be expected at a point on a highway pavement
during the passage of a vehicle.

Consider next a number of vehicles imparting energy
to a point on a highway pavement. If a series of these
vehicles move close enough to each other, the pattern of
the acceleration-time record would demonstrate the super-
position of the individual responses, Fig. 14(a). In
this figure a_1 1 b_1, a_2 2 b_2, a_3 3 b_3 ---, a_n n b_n
represent the accelerations corresponding to the
passage of each of n vehicles. In Fig. 14(b) the solid
curve represents the overall acceleration pattern, obtained
by joining the peaks of the superimposed individual
accelerations; 1 through n_1. In the latter figure, a_1 1 n_1
b_n shows the acceleration-time record for a stream of
vehicles. b_n 1' n_2 b_n' shows the acceleration - time record
for a subsequent stream. The first stream of vehicles had
n_1 number of vehicles and second stream of vehicles had n_2
vehicles. An acceleration - time record such as a_1 1 n
can be designated as a pattern of "uniform acceleration".
One such as the curve representing a_1 1 n_1 b_n 1' n_2
called "Periodic acceleration". Two different laboratory
test procedures, one for uniform acceleration and another
for periodic acceleartion will, therefore, be required
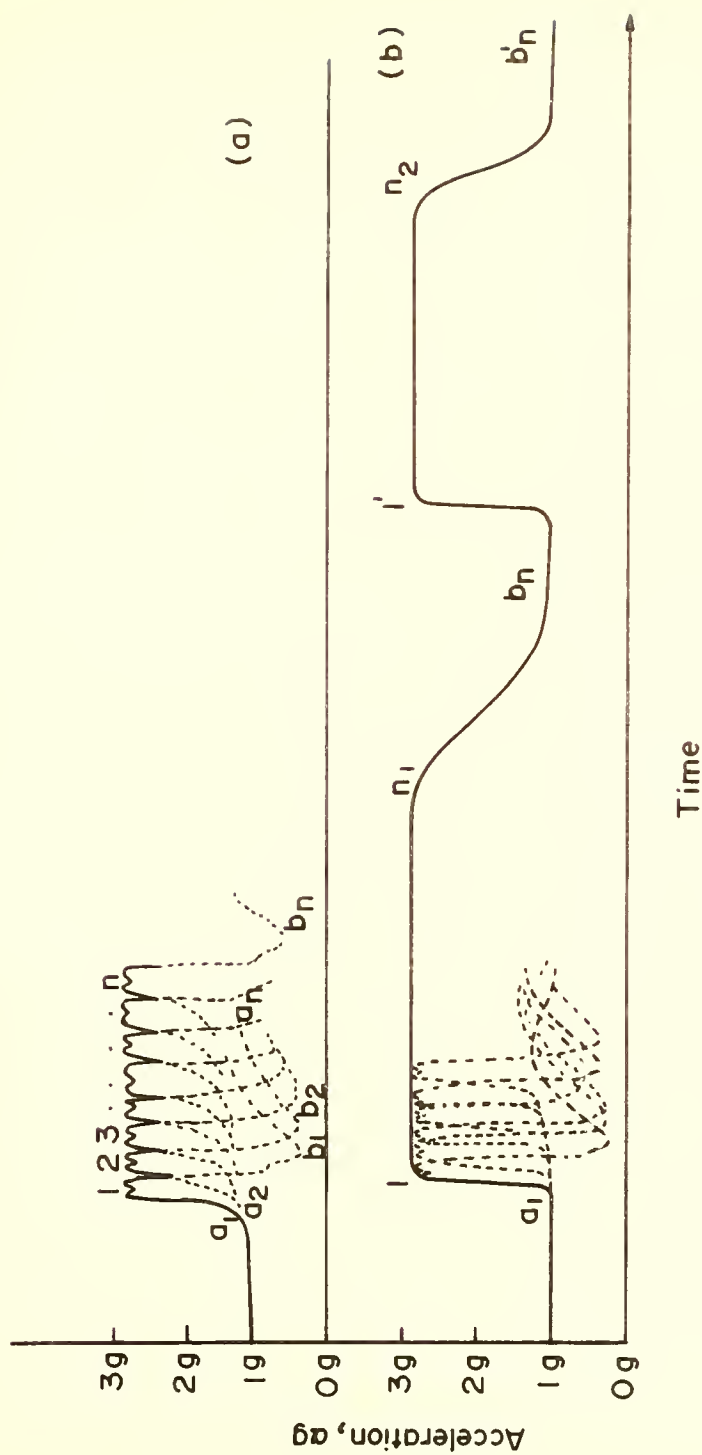to model vehicular action representing these anticipated
field conditions.

FIGURE 14   HYPOTHETICAL ACCELERATION-TIME RECORD FOR A PAVEMENT ELEMENT
SUBJECTED TO COMBINED ACCELERATIONS DUE TO A NUMBER OF
VEHICLES TRANSMITTING ENERGY TO IT.

a) Sheet-Asphalt Samples: Triaxial compression and
hollow cylinder tests were conducted on asphalt cylindrical
samples at different temperature and acceleration fields.

Before the start of the test the cell and the displace-
ment meter were calibrated. Temperature of the testing
chamber (room) could be maintained between 22°C and 45°C.
Some variation in temperature was noted within the room,
but, in general, this variation was less than ± 0.5°C from
the average temperature at the point of measurement. For
test temperatures higher than 45°C the asphalt sample was
kept in a water bath at the desired constant temperature
for 48 hours before the test. After a period of 48 hours
the sample was taken out, wrapped with rubber mem-
brane, placed inside the specimen container and the cell
assembled. The specimen container was then fixed to the
pin on the arm of the centrifuge. The desired confining
pressure was then applied on the specimen. The centrifuge
was rotated and the speed was slowly increased. When the
desired rotational speed (achieved in approximately 15
seconds) was attained the loading operation (axial) was
started until sample failure was registered. This will be
called failure strength under uniform acceleration field.
Temperature measurements of the samples after the test
indicate a maximum drop of 1°C.

A periodic acceleration field was achieved by first
increasing the rotational speed of centrifuge to the
desired level (in less than 15 seconds) and then bringing
the speed to zero level (in about another 15 seconds).
This operation was repeated (at the rate of 2 cpm) during
the loading (axial) period of the sample. The failure
load was intended to represent the effect of periodic (2
cpm) acceleration on the strength of tested sample.

In triaxial compression tests the confining pressure
was applied by gas pressure from the larger gas cylinder
(mentioned previously in the subsection Apparatus) and
failure was brought by increasing the axial load. In the
hollow cylinder tests, outside confining pressure (applied
from the smaller gas cylinder) was maintained constant and
failure was brought by increasing the inside pressure
(applied by controls from larger gas cylinder).

Friction between the ends of the specimen and the
rigid end caps necessary to transmit the axial load re-
stricts lateral deformation adjacent to these surfaces.
This leads to a departure from the condition of uniform
stress and strain. Tests indicate that no significant
error occurs in the strength measurement, provided that
the ratio of length to diameter is about 2 (Bishop and
Henkel, 1964, and Duncan and Seed, 1967). Further, if the
diameters of the lubricated end plates are larger than the
specimen, it will reduce the nonuniformity in stress and

strain (Rowe and Barden, 1964, and Kirkpatrick and Belshaw, 1968). In the triaxial tests that were conducted during this investigation, the length to diameter ratio was always greater than 2 and the diameter of the top loading cap was 0.15 inch more than of the specimen. Hence it is felt that homogeneous stress and strain conditions within the specimen can be reasonably assumed for these tests and no significant error occured in the strength measurement. The deviator stress was calculated in these circumstances on the basis of the average cross-sectional area (Bishop and Henkel, 1964).

b) <u>Samples of Cohesionless Soil</u>: Effect of acceleration on volume change properties of sand was measured by placing a given weight (458.6 gm) of dry sand in a plexiglass cylinder (9.2-cm length and 6.3-cm diameter). The height of fall of the sand (during placement inside the cylinder) was kept constant (about 1.00 inch) by pouring it through a funnel. This plexiglass cylinder, filled with dry sand, was then put inside the specimen container. The specimen container was then fixed to the pin on the arm of the centrifuge. The change in volume of sand was obtained by measuring the change in height of the soil column inside the cylinder after the sand was subjected to an acceleration for a period of 5 minutes.

The effect of confining pressure on the volume change due to the induced accelerations was determined by

subjecting the (above mentioned) sand column to vacuum confinement before and during the time it was subjected to acceleration fields. The placement density at zero confinement was 1.60 gm/cm^2 (e = 0.65).

Triaxial compression tests were performed on 1.5 inch diameter and 3.0-inch high (e = 0.48), dry, sand, cylindrical samples. For each test confining pressure was applied by vacuum. The specimen was subjected to acceleration fields in the centrifuge and failure was brought about by increasing the axial load.

c) Compacted cohesive soil samples: The specimens investigated in this phase of the study were limited to unconfined compression (uniaxial) tests of compacted clay cylinders (γ = 2.14 gm/cm^3).

Before the start of the test the load cell and the displacement meter were calibrated. The sealed compacted sample was taken out and the ends of the sample were lubricated with silicone grease. Two thin rubber membranes separated by a layer of grease were kept between the end platens and sample surface, and a layer of grease was applied to the platen surface. Thus three layers of silicone grease and two membranes separated the ends of the sample from the end platens. This ensured homogeneous stress and strain conditions within the sample during the test (Rowe and Barden, 1964; Duncan and Seed, 1967; and Kirkpatrick and Belshaw, 1968). The sample was then placed inside the specimen container and the cell assembled.

The specimen container was fixed to the pin on the arm of the centrifuge. The centrifuge was then rotated and the speed was increased. When the desired rotational speed was attained the loading (axial) operation was started until sample failure was registered. Water content of the sample after failure was then recorded.

TEST RESULTS

This section summarizes observed test data and computations. The section is divided into sub-sections related to each major area of study.

Sand-Asphalt Samples

The compacted specimens were weighed to the nearest one-hundredth of a gram and the diameter and height determined as an average of at least three measurements. All linear measurements were made to the nearest one hundredth of a centimeter. These measurements provided the initial height and volume values of the specimen upon which all computations were based.

Densities of sand-asphalt samples were recorded both before and after they were subjected to acceleration fields in the centrifuge. For all practical purposes the change in density with acceleration was negligible.

Stress-Strain Relationships

Loads were applied to the specimen by a strain controlled method. Preliminary tests indicated that volume changes occurred under load to such a degree that an adjustment of the specimen area was required for the

computation of applied stress. This adjustment was made on the assumption that even though the specimen changed volume it would retain a uniform cylindrical shape.

Typical stress-strain curves are illustrated in Figure 15 for one of the test series at different acceleration fields. Figure 16 shows similar data for different confining pressures.

Strength Variation with Acceleration Fields

i) <u>Uniform accelerations</u>. Unconfined compression tests were performed on 1" diameter and 2" high asphaltic concrete cylindrical samples. For each set of tests, temperature (T), initial density (γ_i) and rate of strain ($\dot{\epsilon}$) were maintained constant and acceleration fields, αg, were varied over a wide range of values. Fig. 17 shows the variation of unconfined compressive strength (q_u) with acceleration ratio, α, (other parameters, e.g., T, γ_i and $\dot{\epsilon}$ being constant). Another set of unconfined compressive strength results versus acceleration, αg, for three temperatures (T = 80.6°F, 100°F and 105°F) are shown as data points in Fig. 18. Fig. 19 exhibits the effect of confining pressures on the strength versus acceleration plot at a constant temperature. In each case a loss in strength is recorded with increasing acceleration. However, after a certain critical value of acceleration is reached, the trend is reversed and some strength is regained.
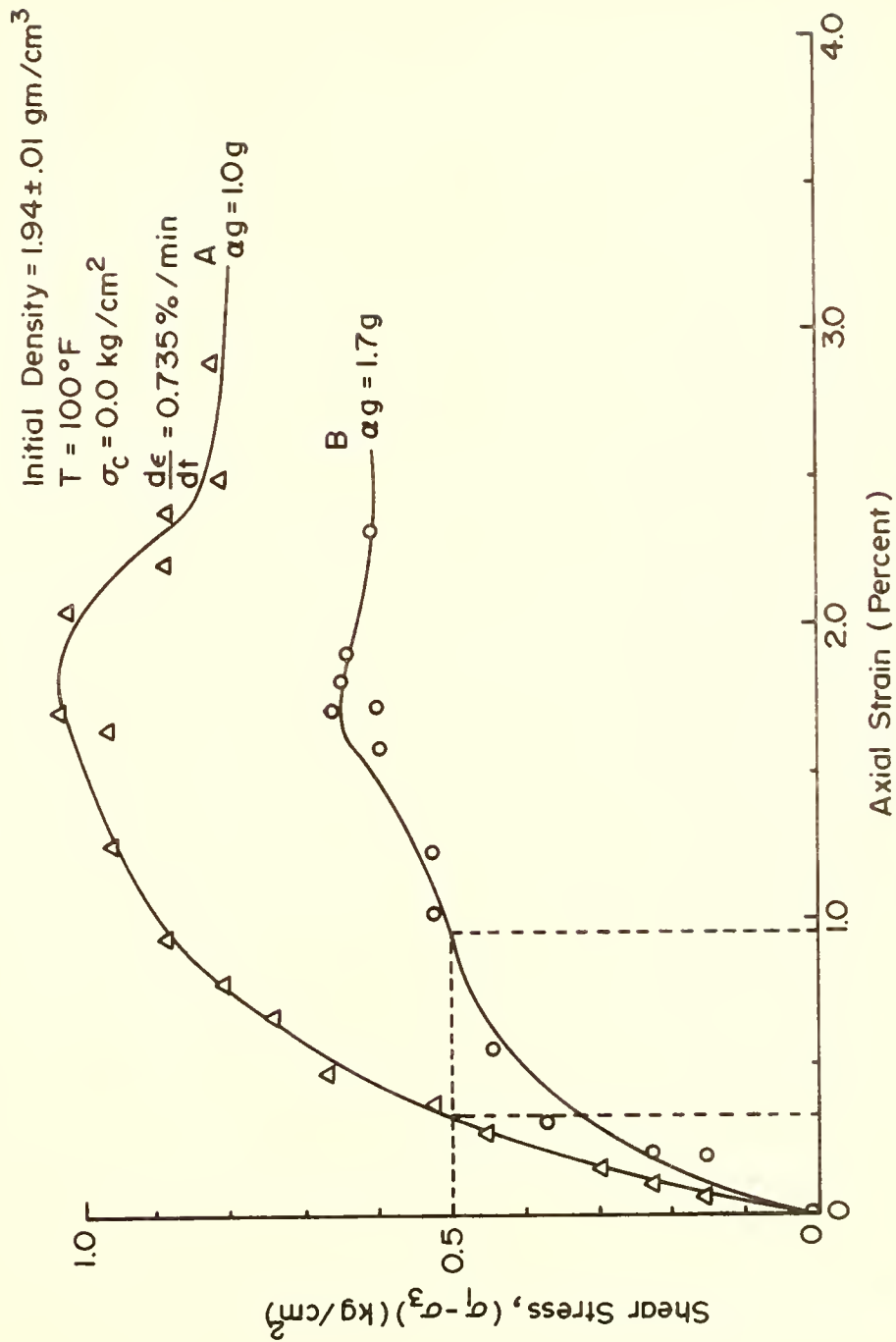
FIGURE 15 STRESS-STRAIN RELATIONSHIPS FOR SAND-ASPHALT SAMPLES AT DIFFERENT ACCELERATIONS.
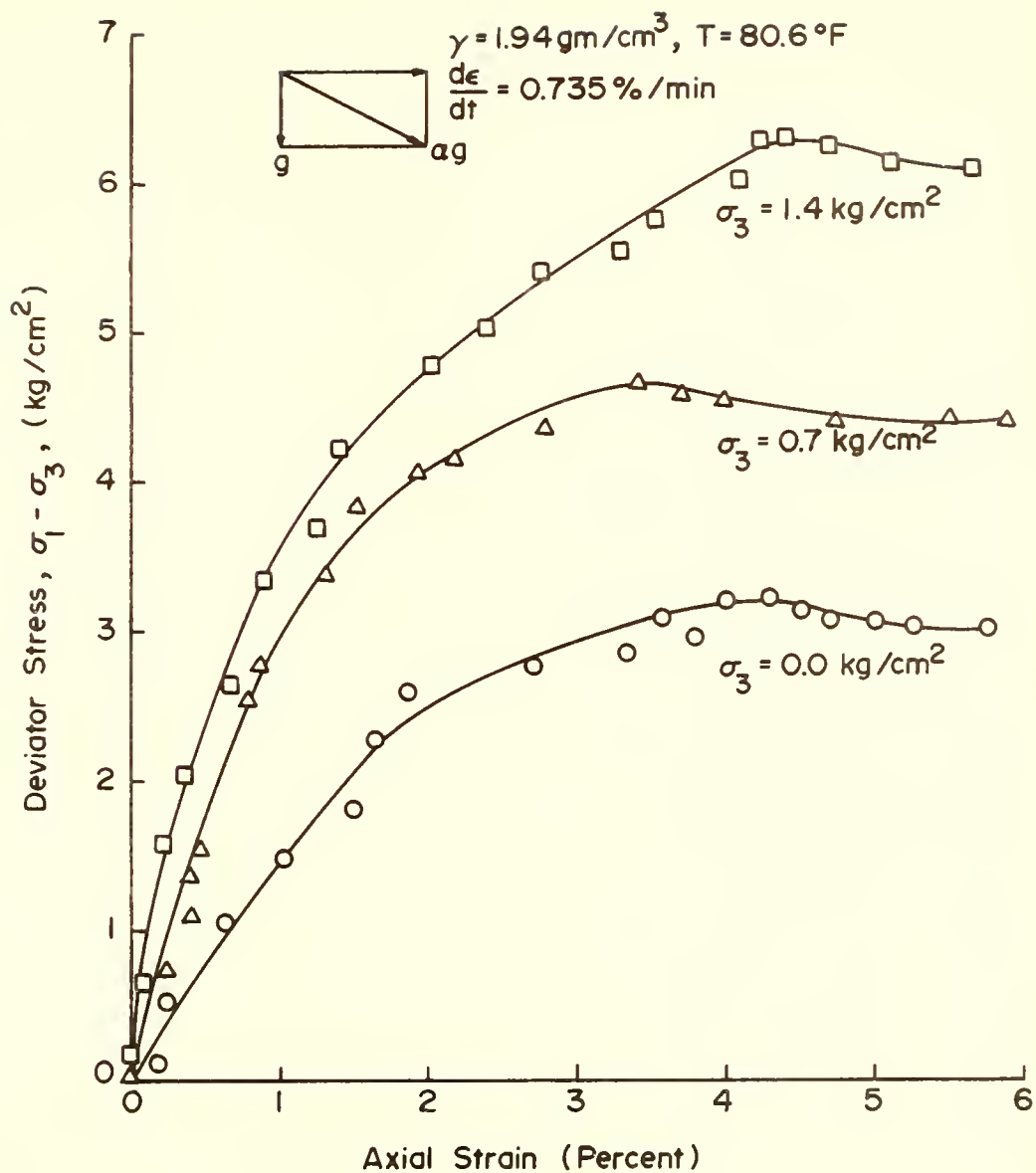
FIGURE 16 STRESS-STRAIN PLOTS FOR SAND-ASPHALT MIX AT DIFFERENT CONFINING PRESSURES (ag = lg).
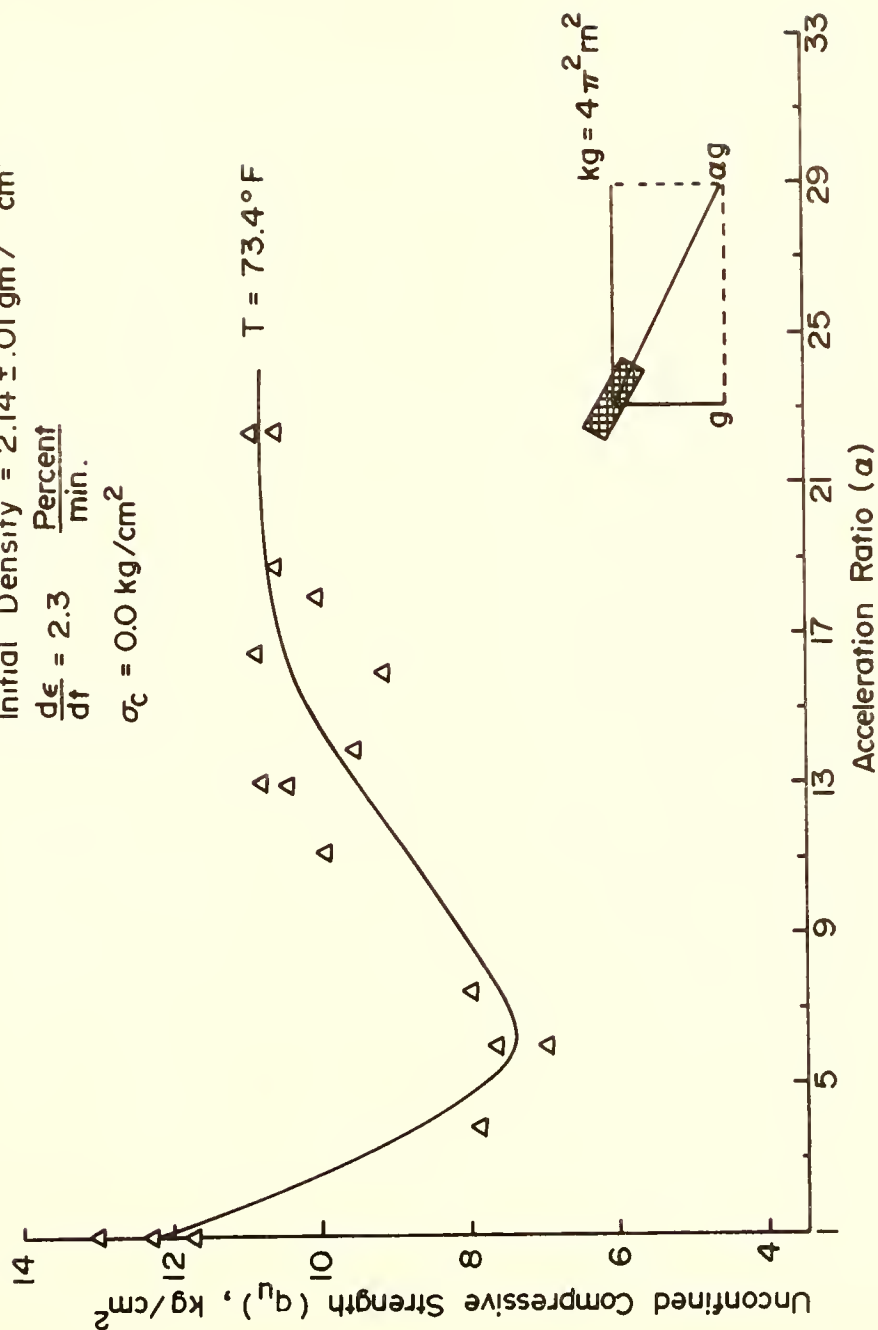
FIGURE 17 UNCONFINED STRENGTH VARIATION WITH UNIFORM ACCELERATION CHANGE OF SAND ASPHALT SAMPLES.
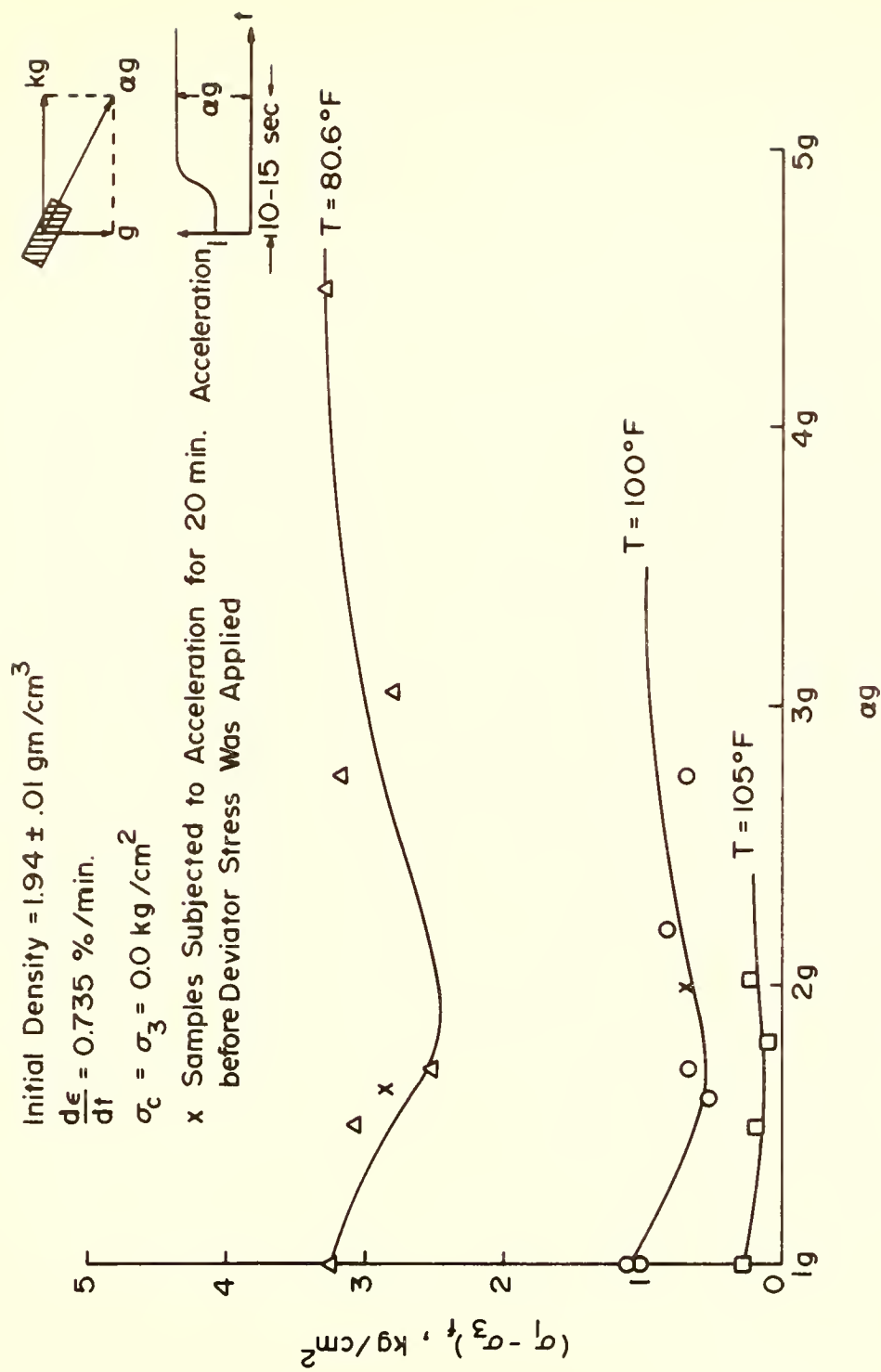
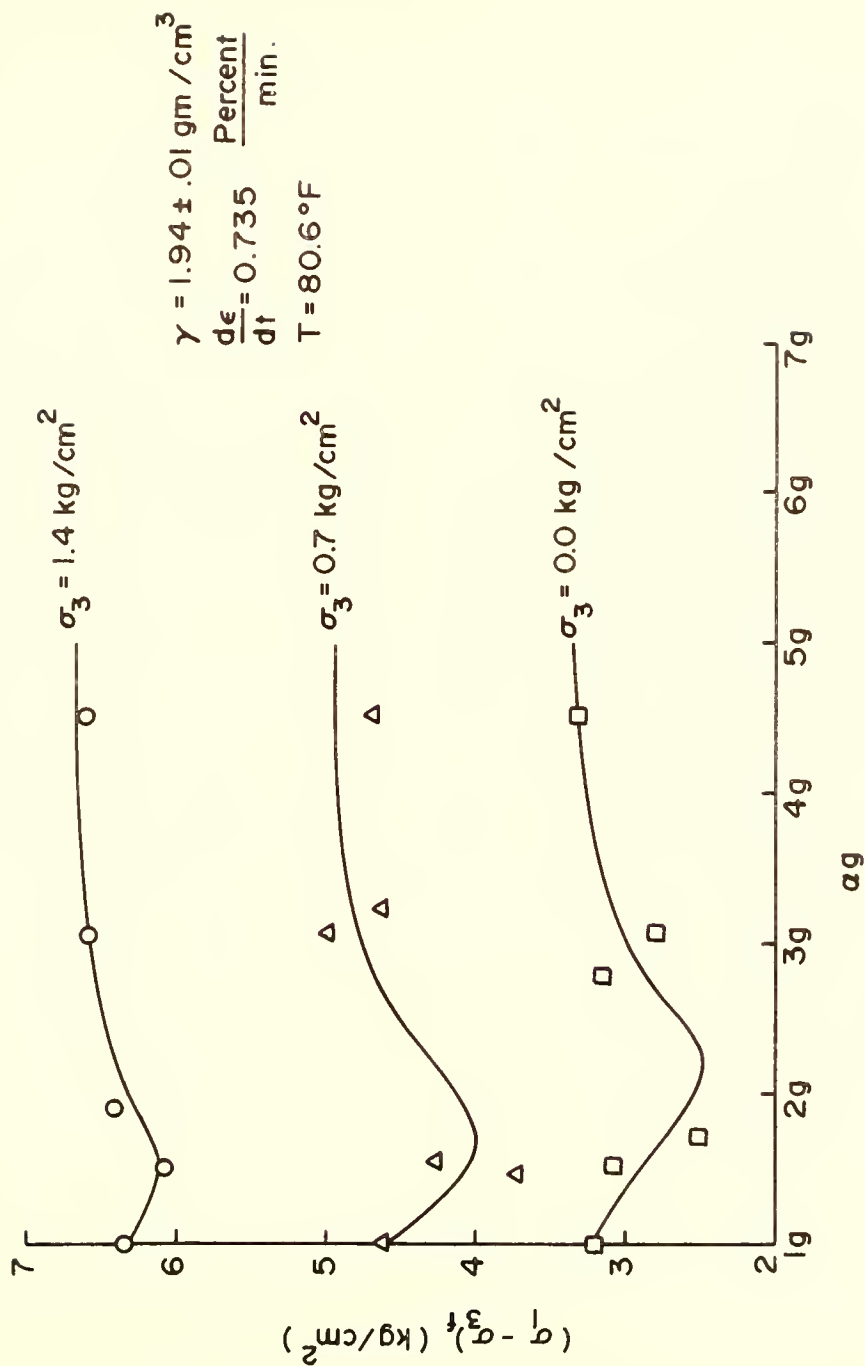FIGURE 18 UNCONFINED STRENGTH VARIATION WITH UNIFORM ACCELERATION FOR SAND ASPHALT SAMPLES.

FIGURE 19 EFFECT OF CONFINING PRESSURES ON THE STRENGTH VARIATION WITH ACCELERATIONS (SAND-ASPHALT SAMPLES).

In Fig. 20 is shown the general pattern of strength change (as a percentage), experienced at different temperatures and confining pressures, plotted as a function of resultant acceleration to which the specimen is subjected during testing. Fig. 21 demonstrates the influence of temperature and confining pressures on critical accelerations.

ii) <u>Periodic Nature of accelerations</u>. Periodic accelerations were applied by increasing the acceleration linearly to a certain level, αg, and then reducing it to $1g$. This process was repeated at a frequency of 2 cycles per minute. Fig. 22 shows the resulting unconfined compressive strength (q_u) versus periodic acceleration, αg, at different temperature levels. Fig. 23 exhibits the effect of initial density on the typical q_u versus αg plot whereas Figs. 24 and 25 show the effect of confining pressures in this plot. In Figs. 26 and 27 are shown the general pattern of strength loss (as a percentage), experienced at each of the test temperatures, plotted as a function of periodic acceleration to which the specimen is subjected during unconfined compression testing.

Hollow cylinder tests were also conducted to find the effect of intermediate principal stresses on strength parameters at different acceleration fields. Tests were conducted on 3" high asphalt samples of 1.5" outer
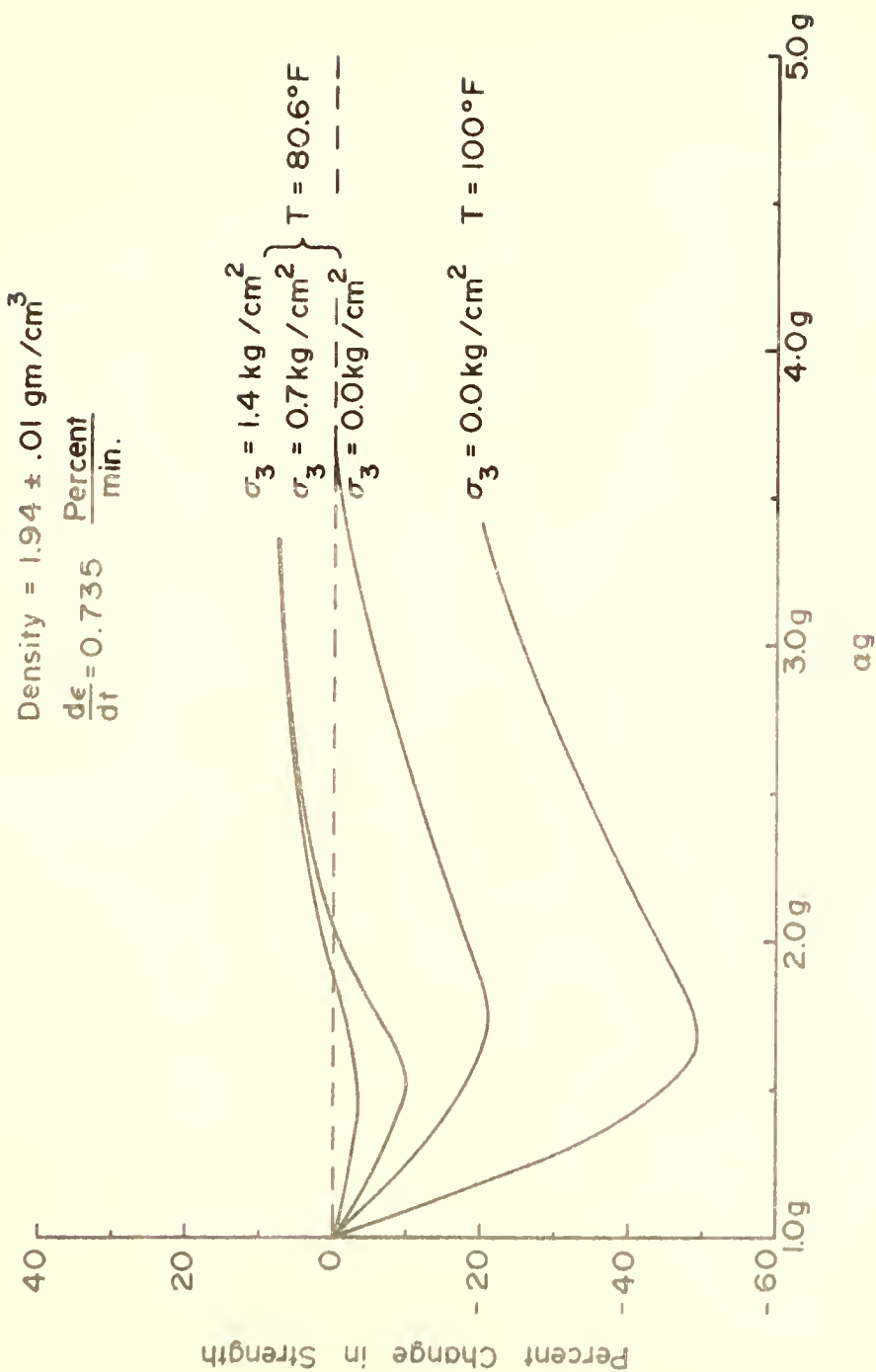
FIGURE 20 PERCENT STRENGTH CHANGE WITH **UNIFORM** ACCELERATION (SAND-ASPHALT SAMPLES).
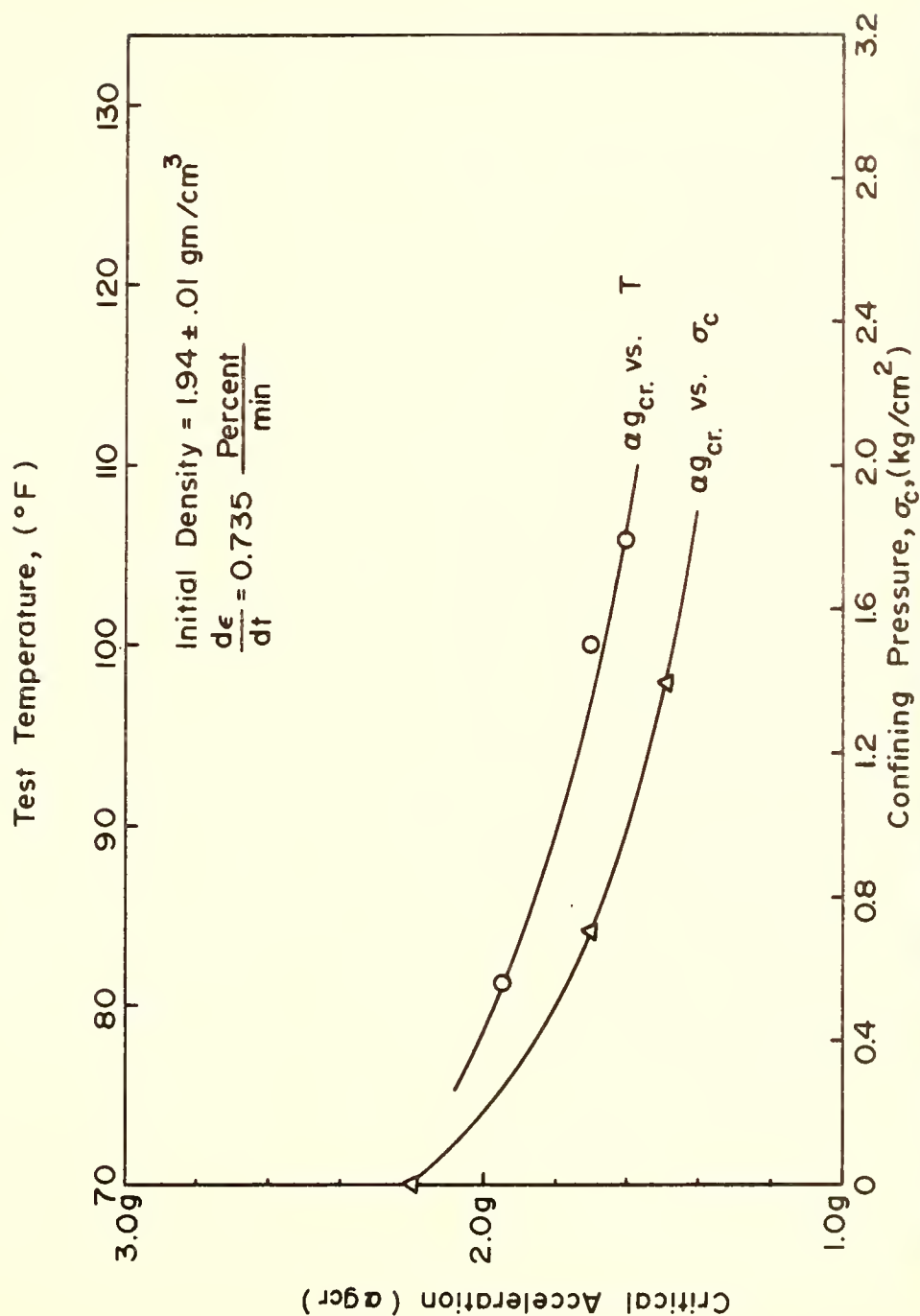
FIGURE 21 EFFECT OF TEMPERATURE AND CONFINING PRESSURE ON CRITICAL ACCELERATION (SAND ASPHALT SAMPLES).
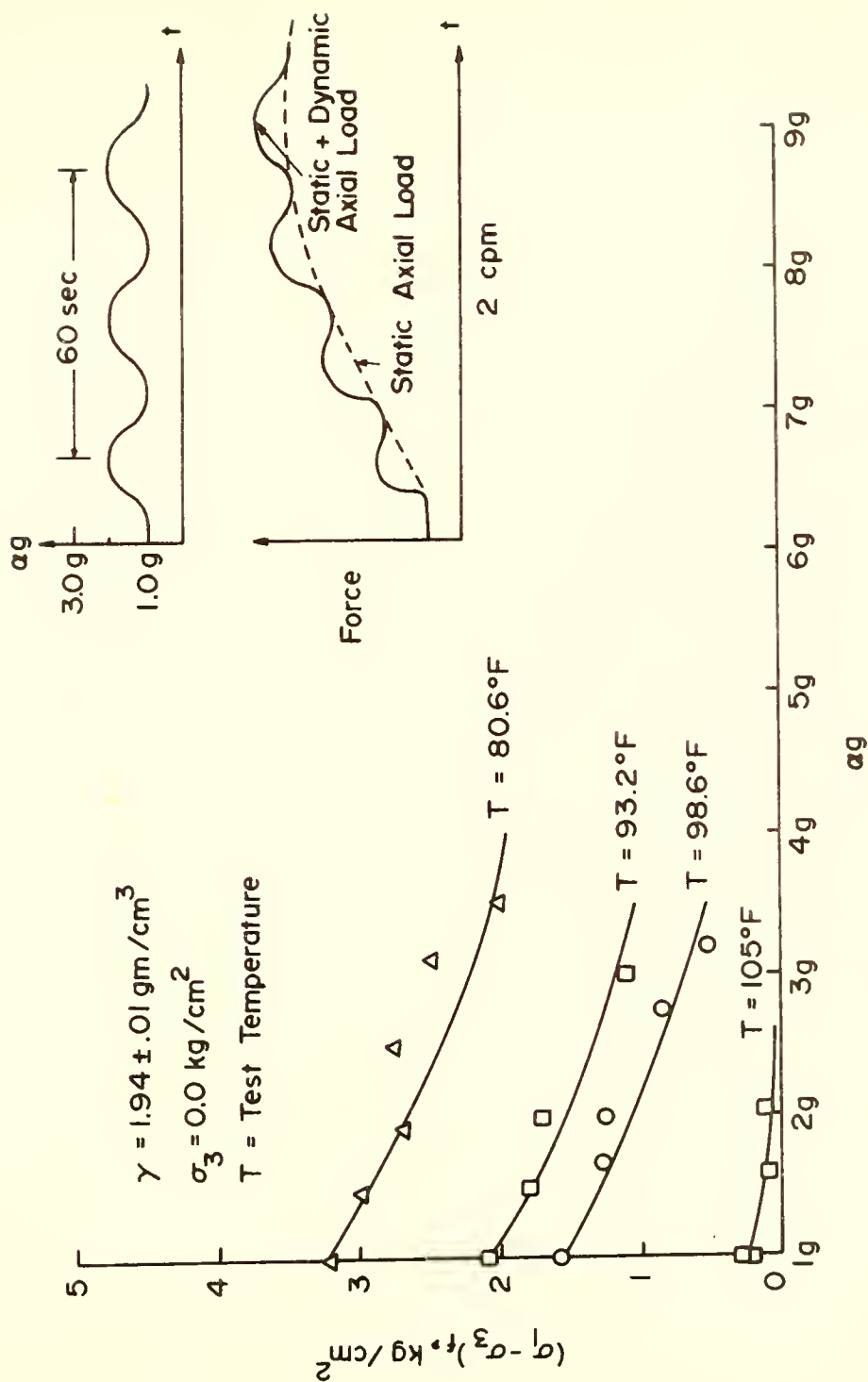
FIGURE 22 UNCONFINED COMPRESSION STRENGTH OF SAND ASPHALT SAMPLES UNDER PERIODIC ACCELERATION FIELDS.
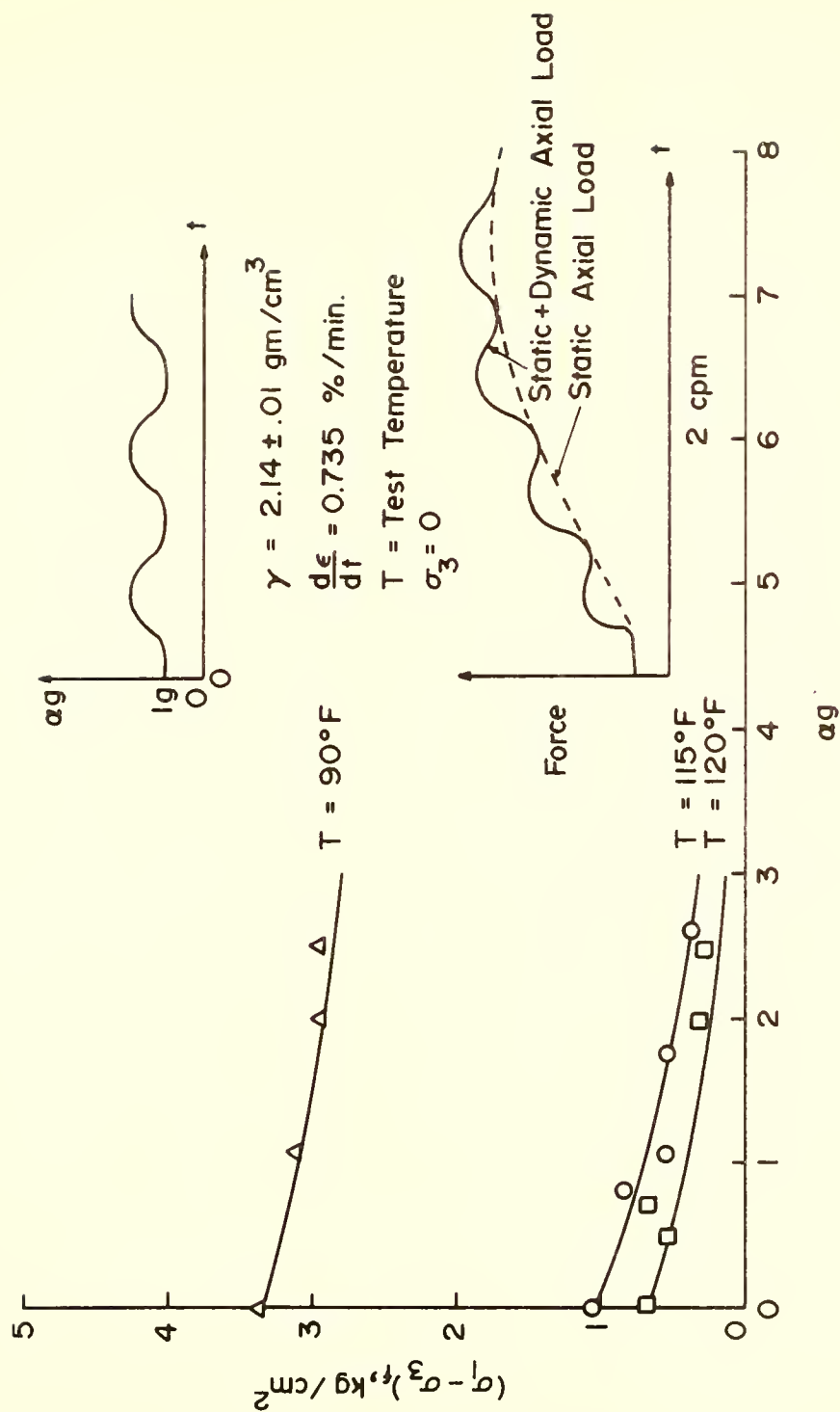
FIGURE 23 UNCONFINED COMPRESSION TESTS OF SAND ASPHALT SAMPLES UNDER PERIODIC ACCELERATION FIELDS.
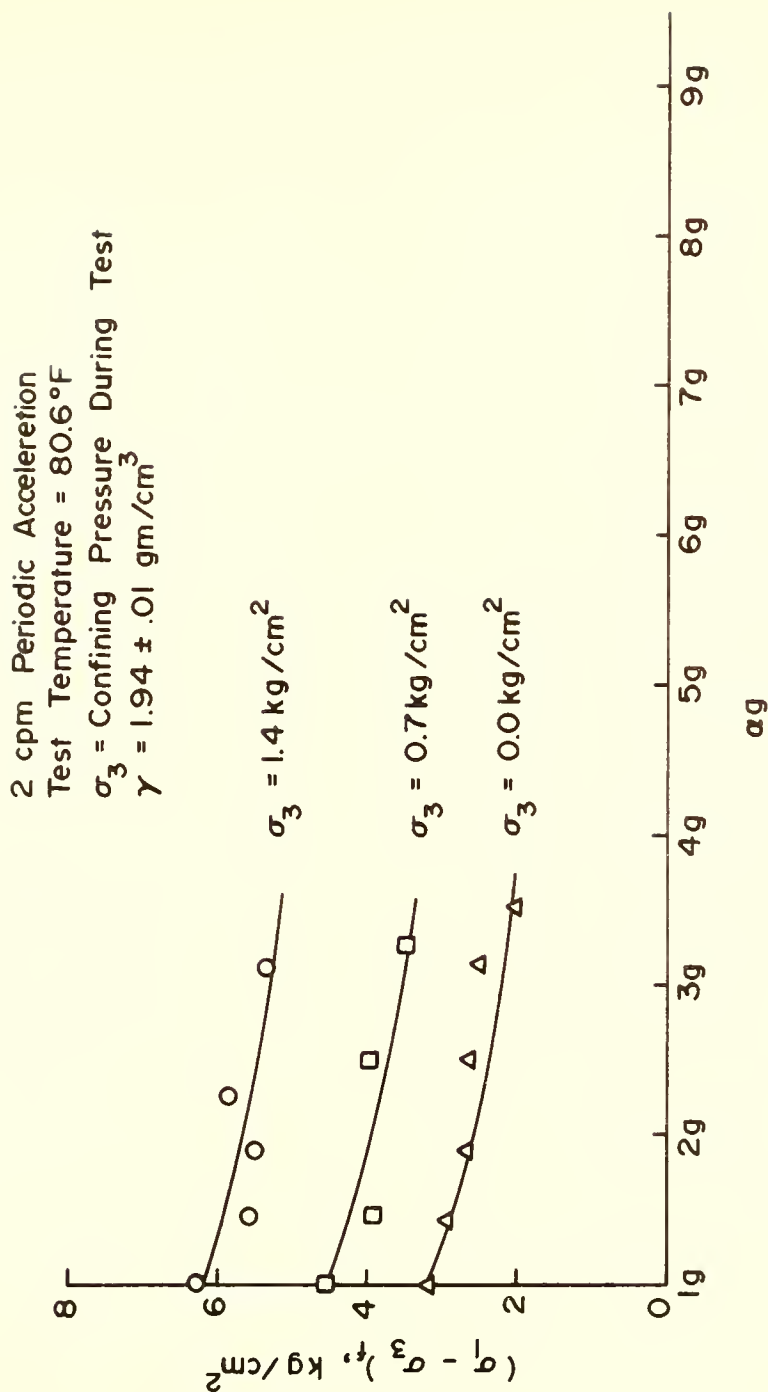
FIGURE 24 CONFINED COMPRESSION TESTS OF SAND ASPHALT SAMPLES UNDER PERIODIC ACCELERATION FIELDS.
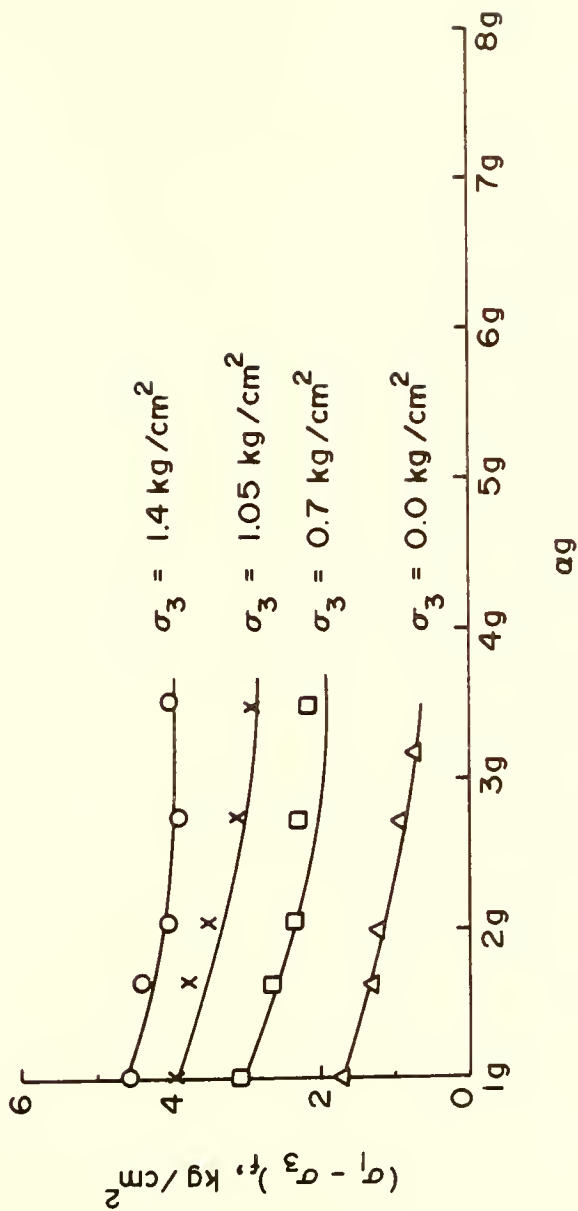
FIGURE 25 CONFINED COMPRESSION TESTS OF SAND ASPHALT SAMPLES UNDER PERIODIC ACCELERATION FIELDS.
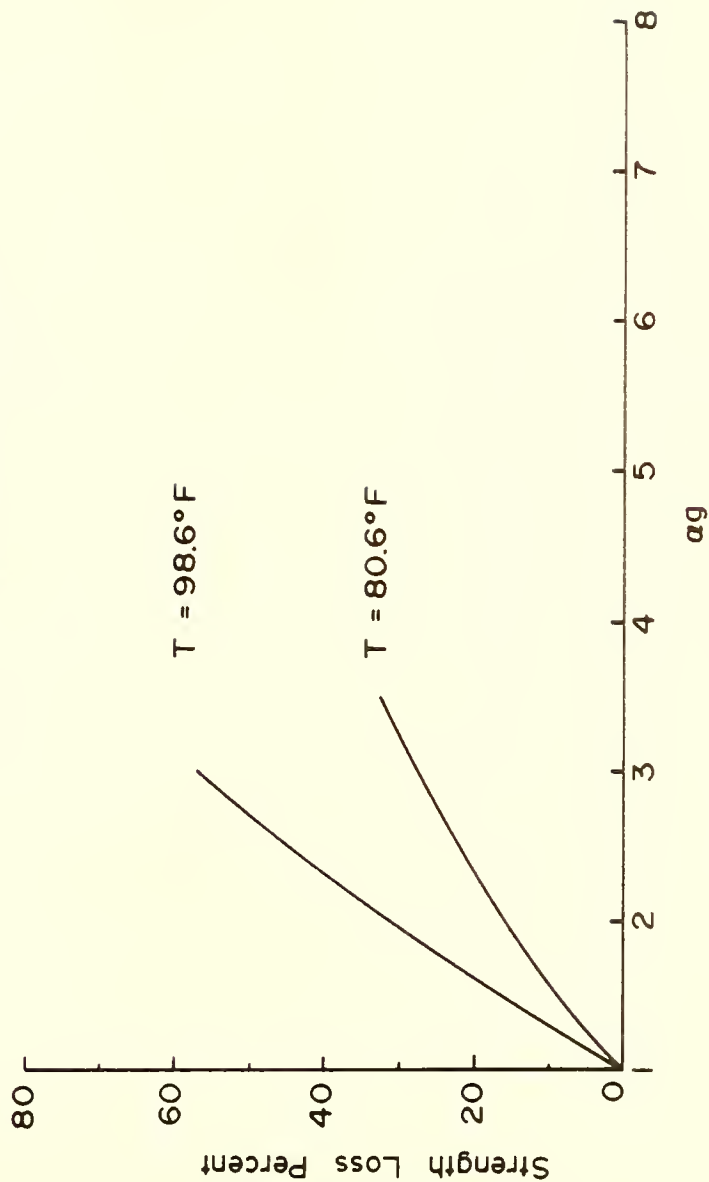
FIGURE 26 STRENGTH LOSS DUE TO ACCELERATION AT DIFFERENT TEMPERATURE LEVELS (SAND-ASPHALT SAMPLES).
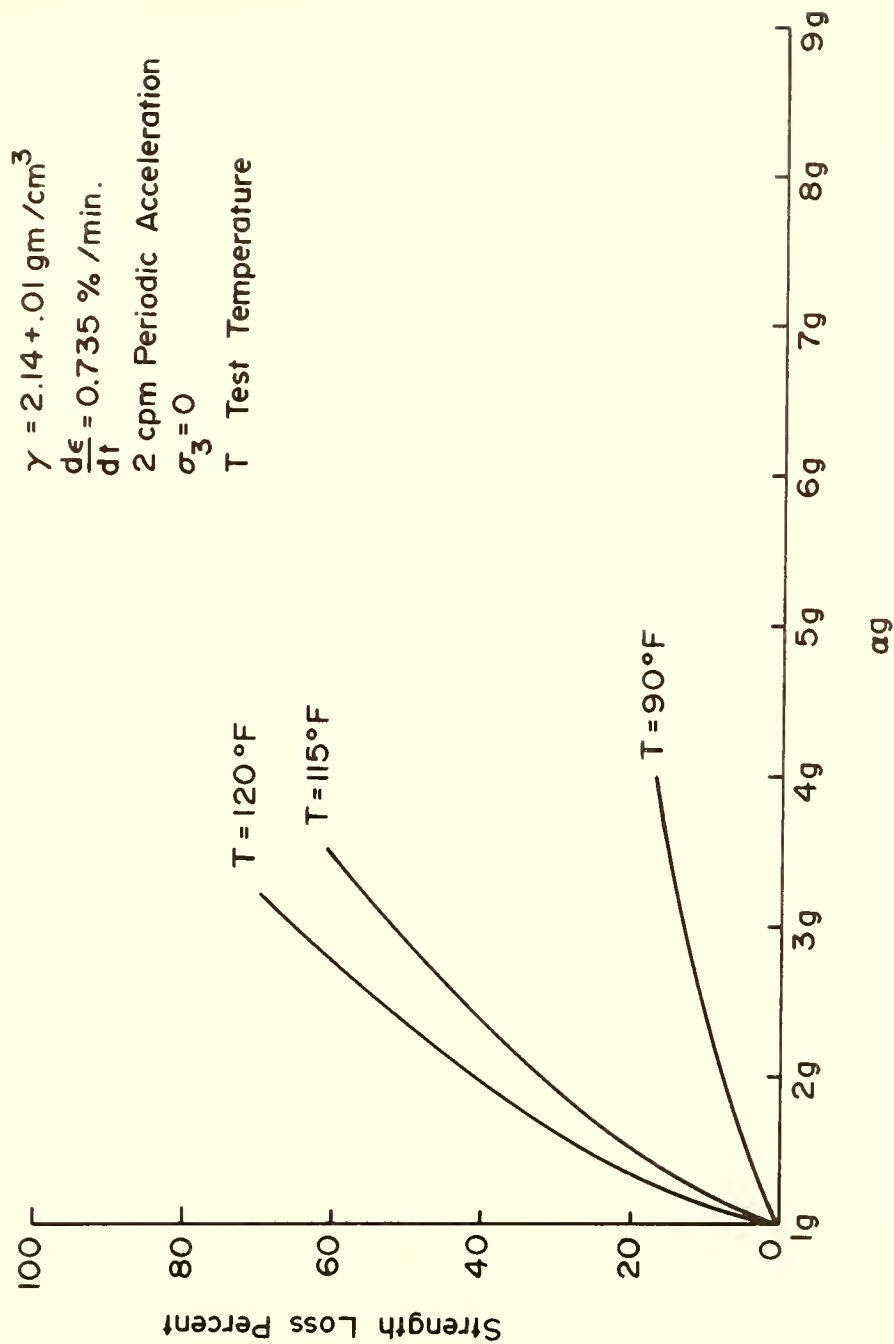
FIGURE 27 STRENGTH LOSS DUE TO ACCELERATION AT DIFFERENT TEMPERATURE LEVELS (SAND-ASPHALT SAMPLES).

diameter and 0.5" internal diameter. Failure was brought by increasing the inside pressure (p_i) keeping outside pressure (p_o) constant. The three principal stresses at failure were calculated by relations A-3, A-4 and A-5 (Appendix A).

Tables 3 and 4 summarize the test results of hollow cylinder tests conducted at two different acceleration levels. Figs. 28 and 29 present the resulting Mohr-Coulomb failure envelopes. Test data for triaxial and hollow cylinders are also plotted in these figures. Appendix B explains the method of projection of test data onto octahedral plane.

Fig. 30 presents a graphical summary of the values of observed shear strength parameters, "c" and "ϕ", at failure for various acceleration fields. Also shown in this figure are the results (c and ϕ) obtained from hollow cylinder tests. In general, c and ϕ parameters both decrease with increasing accelerations.

Cohesionless Soil

Experiments were conducted to determine the effect of accelerations on the change in void ratio of cohesionless soils. Changes in void ratios, due to changes in acceleration, were measured by placing the dry cohesionless soil in a plexiglass cylinder (9.2 cm. long, 6.3 cm. diameter) and then subjecting it to an acceleration field in the

Table 3a. Hollow Cylinder Test Results
($T = 80.6°F$, $\alpha g = 1g$).

Test No.	P_o Kg/cm^2	P_i Kg/cm^2	σ_r Kg/cm^2	σ_a Kg/cm^2	σ_θ Kg/cm^2
1	0	1.96	0	-0.24	-1.16
2	0.70	3.50	0.70	0.35	-0.94
3	1.05	4.34	1.05	0.63	-0.86
4	1.40	4.90	1.40	0.96	-0.74

Table 3b. Comparison of Triaxial and Hollow
Cylinder Strength Parameters

Kind of Test	c	ϕ
Triaxial	0.85 Kg/cm^2	31°
Hollow Cylinder	1.05 Kg/cm^2	33.5°

Table 4a. Hollow Cylinder Test Results
(T = 80.6°F, αg = 2.5g).

Test No.	p_o Kg/cm^2	p_i Kg/cm^2	σ_r Kg/cm^2	σ_a Kg/cm^2	σ_θ Kg/cm^2
1	0	1.89	0	-0.24	-1.15
2	0.7	3.36	0.7	0.37	-0.92
3	1.05	4.06	1.05	0.67	-0.79
4	1.40	4.76	1.40	0.98	-0.68

Table 4b. Comparison of Triaxial and Hollow
Cylinder Strength Parameters.

Kind of Test	c	ϕ
Triaxial	0.75 Kg/cm^2	28.5°
Hollow Cylinder	0.99 Kg/cm^2	29.0°
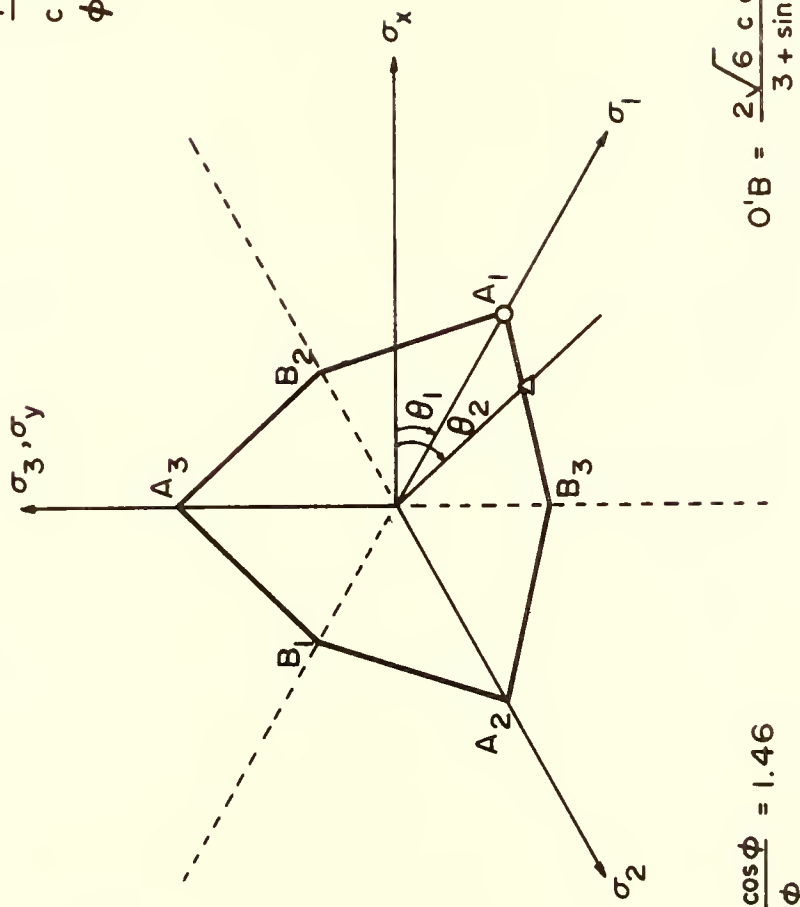
FIGURE 28 MOHR-COULOMB YIELD SURFACE ON DEVIATORIC PLANE $\sigma_1 + \sigma_2 + \sigma_3 = 0$ FOR SAND ASPHALT SAMPLES.
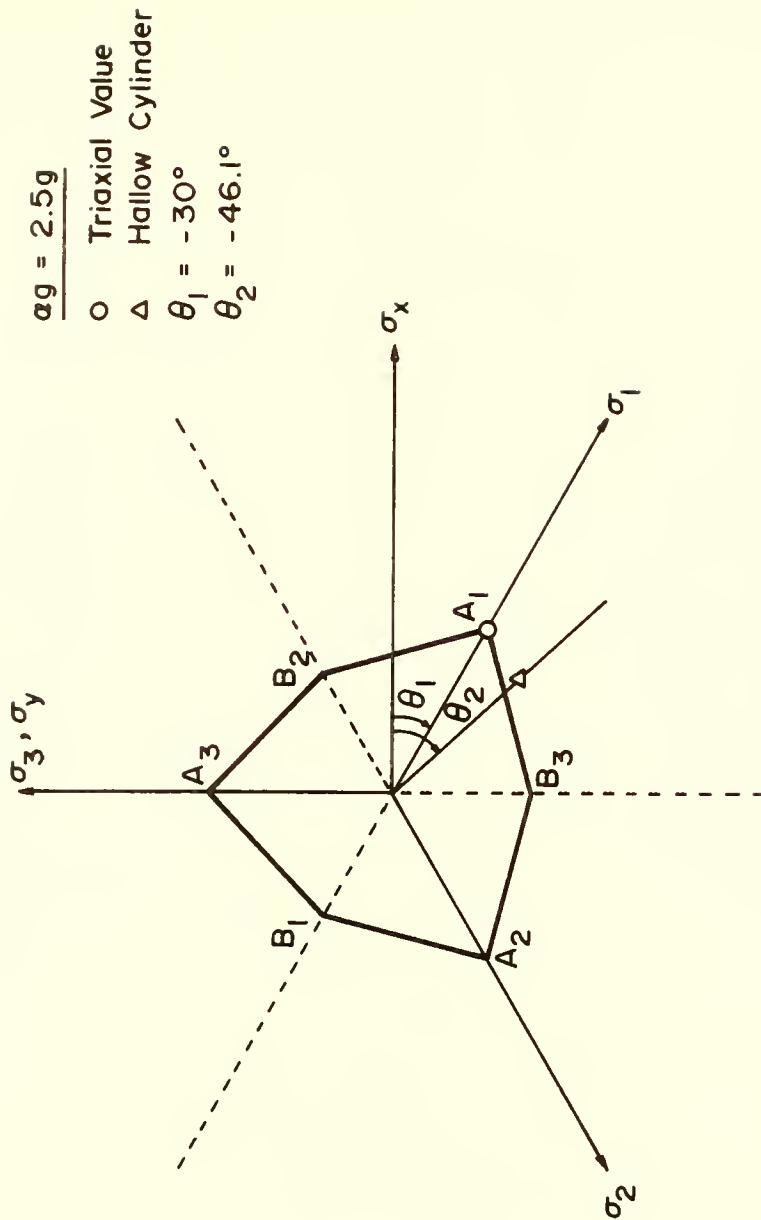
FIGURE 29 MOHR-COULOMB YIELD SURFACE ON DEVIATORIC PLANE $\sigma_1 + \sigma_2 + \sigma_3 = 0$ FOR SAND ASPHALT SAMPLES.
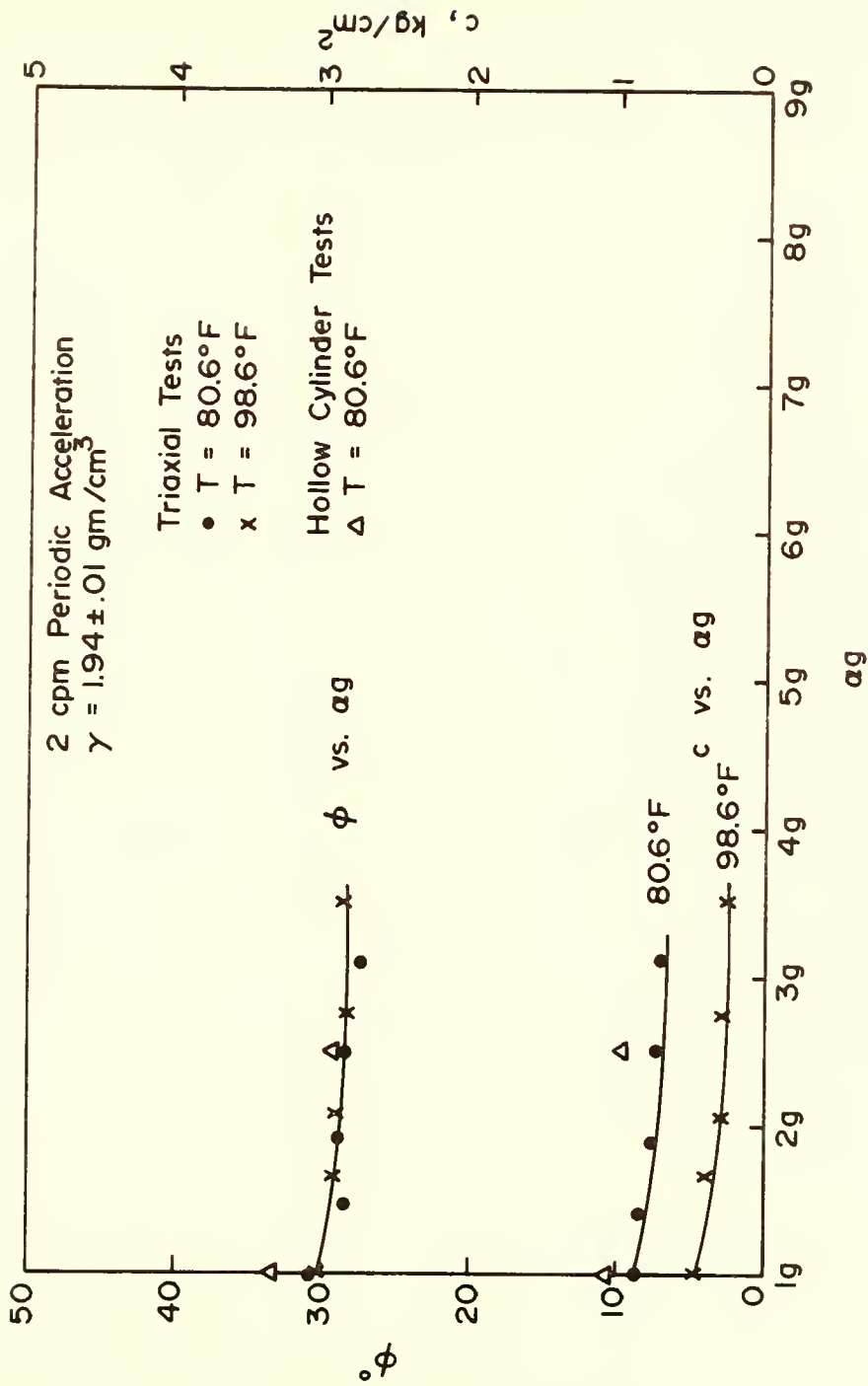
FIGURE 30 PARAMETER c AND φ VARIATION WITH ACCELERATION FIELDS FOR SAND ASPHALT SAMPLES.

centrifuge. The effect of confining pressure on the void ratio, with acceleration, was determined by subjecting the above mentioned sand column to vacuum confinement before and during the time it was subjected to acceleration fields. Figure 31 shows the resulting changes in void ratio with accelerations. Tests were performed at three confining pressures, $\sigma_{c_1} = 0.0$ kg/cm^2, $\sigma_{c_2} = 0.37$ kg/cm^2, and $\sigma_{c_3} = 0.77$ kg/cm^2. All the three sets of test results indicate a decrease in void ratio with increasing acceleration fields. In Figure 32 is shown the relative void ratio (as a percent) as a function of acceleration.

Triaxial compression tests were performed on 1.5 inch diameter and 3 inch high dry sand cylindrical samples. For each test the confining pressure, σ_c, was maintained constant and the acceleration fields, αg, were varied. Fig. 33 shows the variation of deviator stress at failure with acceleration. Results indicate a slight initial increase in compressive strength with increasing acceleration. Volume change measurements during shear were a complex problem in centrifuge apparatus therefore they were not measured.

Cohesive Soil

Unconfined compression tests were performed on 1 inch diameter and 2 inch high samples of compacted cohesive soil. The soil was compacted by static compaction method at 21.2 ± 0.2% compaction water content. The standard Proctor optimum moisture content for this soil was 21.5%. Acceleration
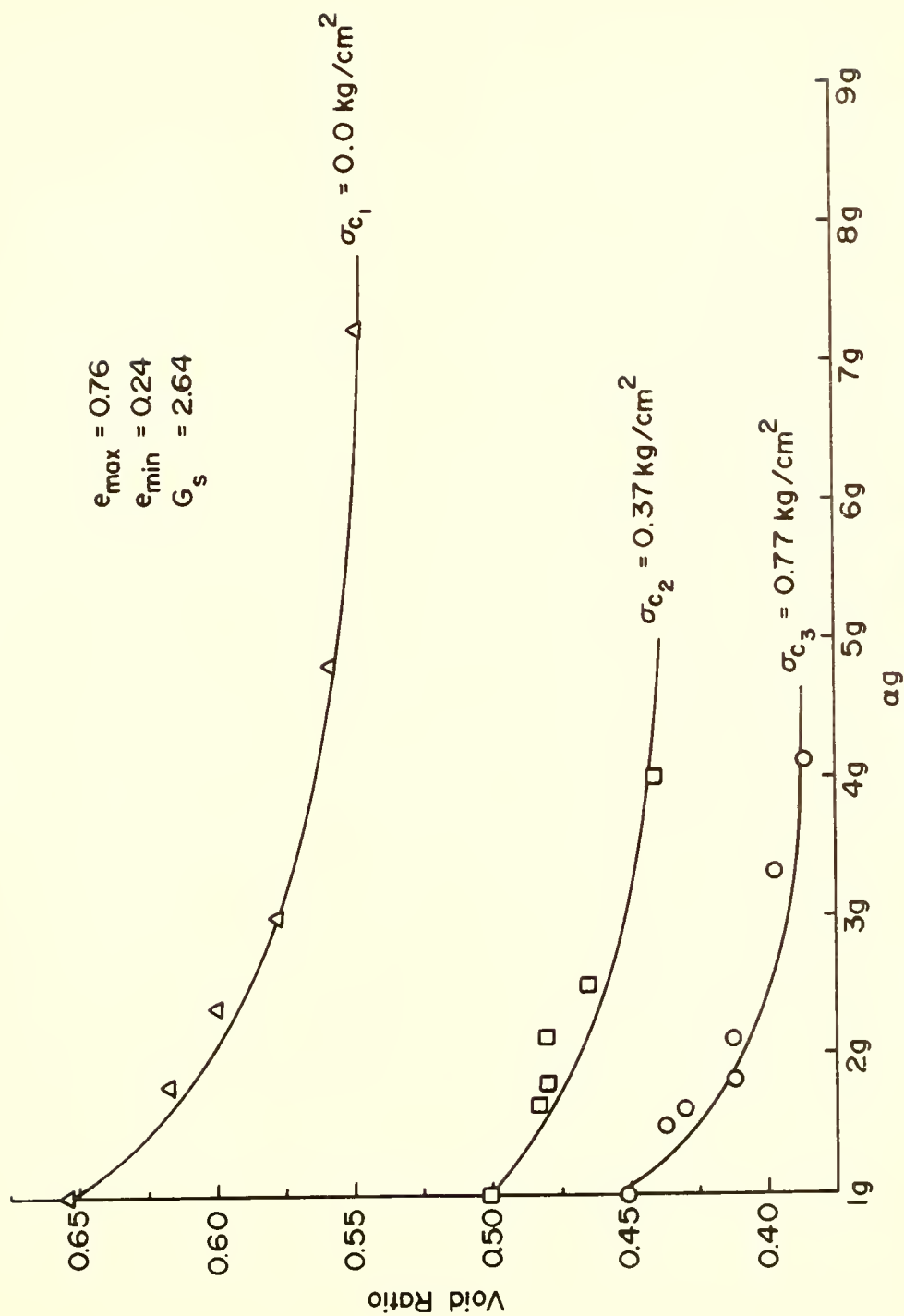
FIGURE 31 VOID RATIO VARIATION OF SAND WITH UNIFORM ACCELERATION.
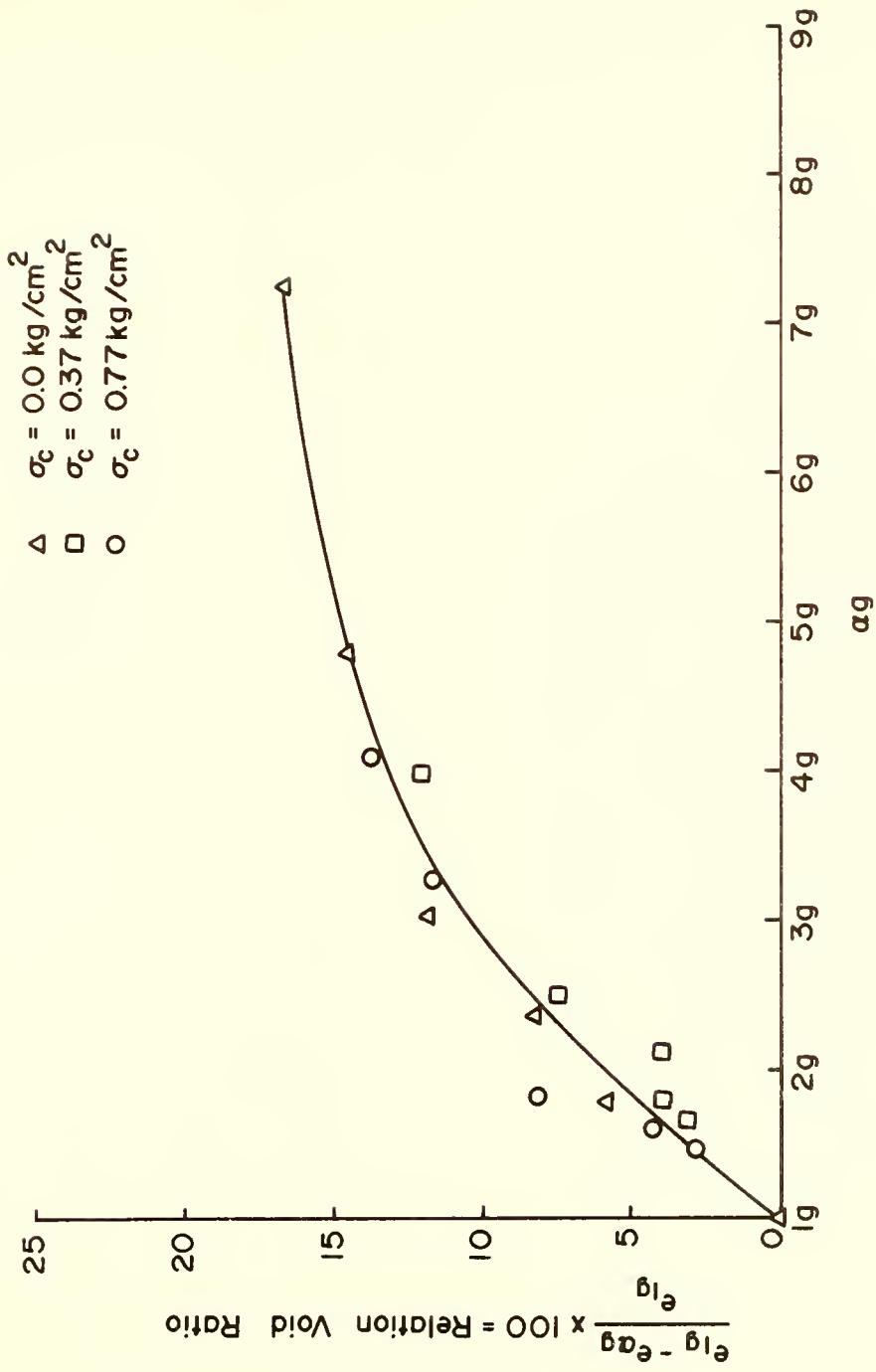
FIGURE 32 RELATIVE VOID RATIO CHANGE OF SAND WITH ACCELERATION.
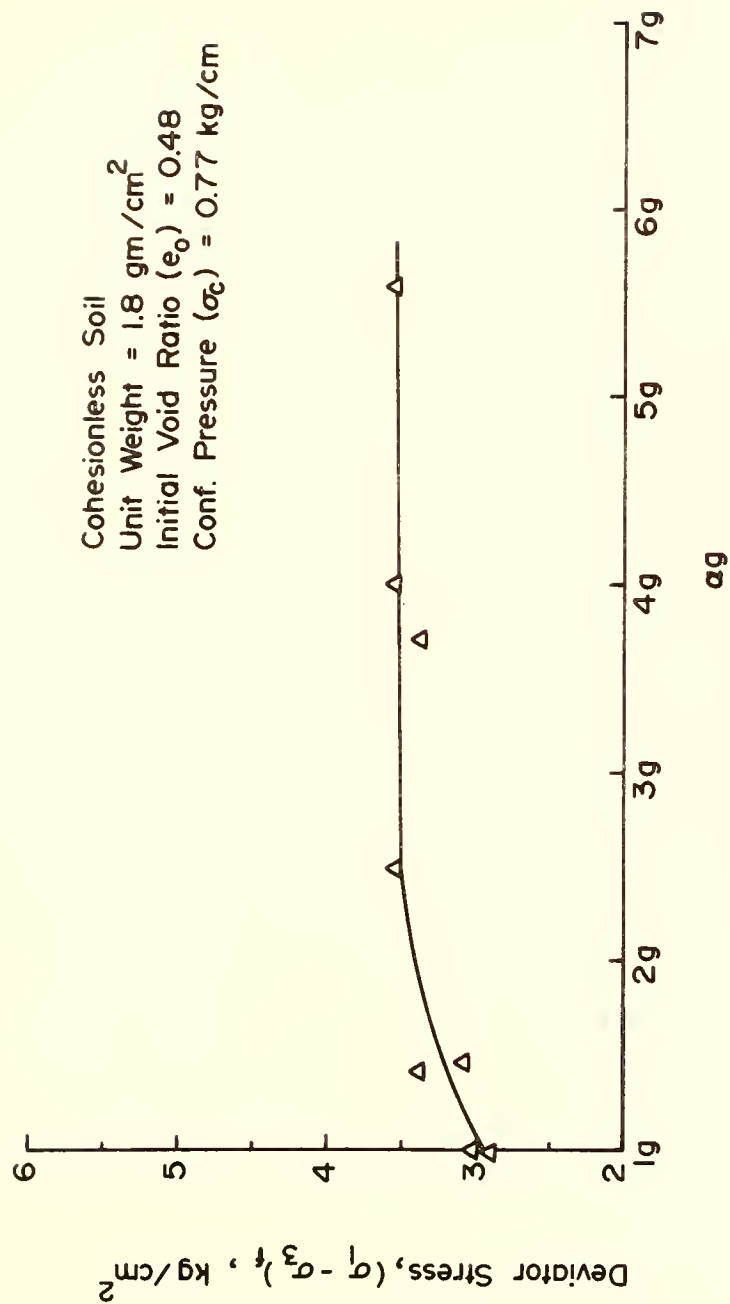
FIGURE 33 STRENGTH VARIATION WITH UNIFORM ACCELERATION CHANGE FOR SAND SAMPLES.

fields, αg, were varied over a wide range of values. Fig. 34 exhibits the typical stress-strain curves for the samples at two different acceleration fields, e.g., $\alpha g = 1.0g$ and $\alpha g = 7.0g$. In this figure (34), it is observed that the initial slope of the stress-strain curves and the failure strength for samples at $\alpha g = 7.0g$ is lower than that for the sample tested at $\alpha g = 1.0g$. The resulting unconfined compressive strength (q_u) versus acceleration field, αg, are shown as data points in Fig. 35. In each case, at first, a loss in strength is recorded with increased acceleration, with the strength eventually approaching an asymptote at about sixty percent of the static unconfined strength.
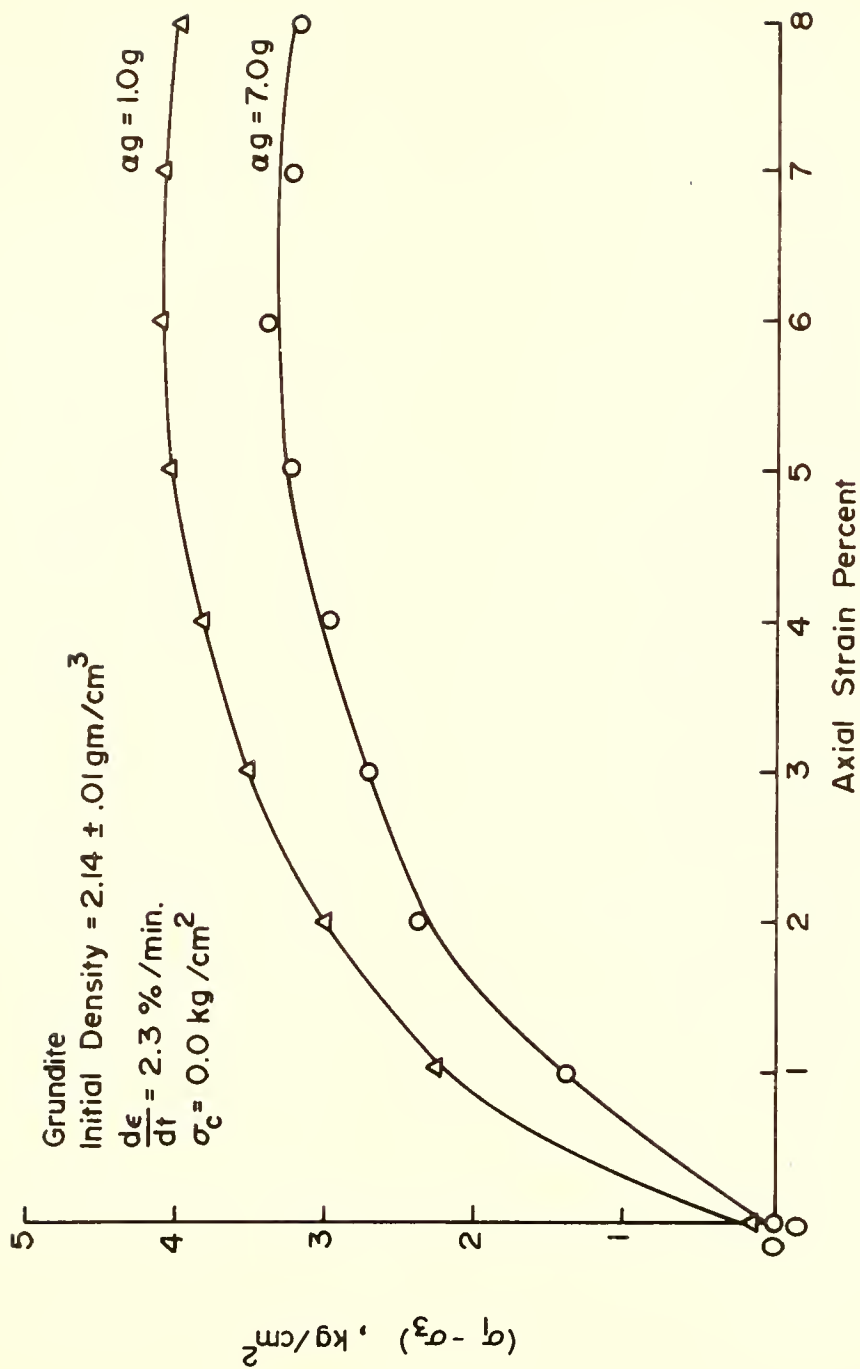
FIGURE 34   STRESS-STRAIN RELATIONSHIP FOR CLAY SAMPLES AT TWO DIFFERENT ACCELERATION FIELDS.
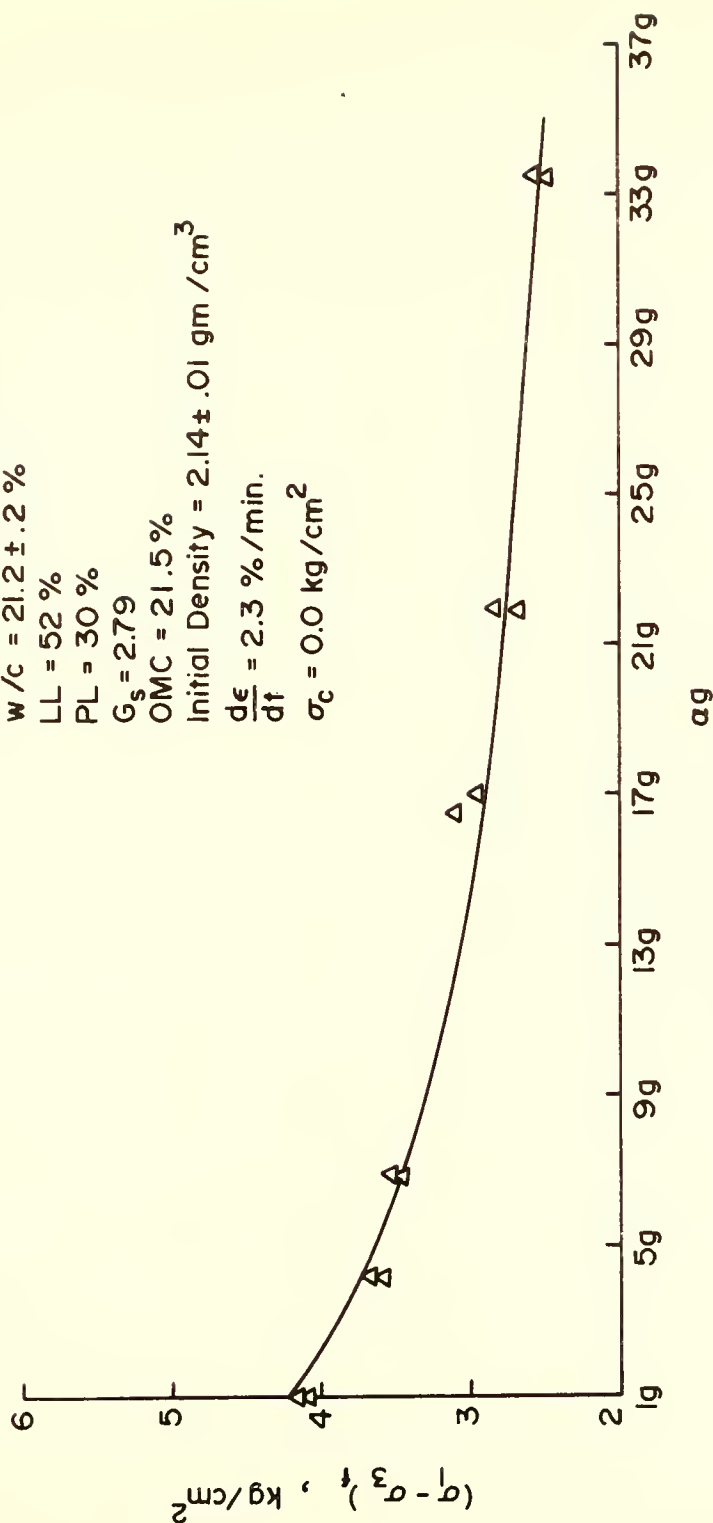
FIGURE 35 UNCONFINED COMPRESSIVE STRENGTH VARIATION WITH UNIFORM ACCELERATION CHANGE FOR CLAY SAMPLES.

DISCUSSION OF TEST RESULTS

The main objective of this research was to determine significant and necessary basic properties of some common materials used in highways. In the section entitled "Background and Significance of Work" it was noted that, if accelerations are ignored, the parameter c, ϕ and γ are sufficient to characterize a material. However, theory indicated that these parameters were not sufficient for material characterization if accelerations could not be neglected. Any study to determine significant and necessary basic properties of materials must, therefore, include the determination of the effect of accelerations on material properties. This was the underlying purpose of the present study.

Before interpreting the results of triaxial and plane strain tests, it is desirable to correct the test data for the loads carried by rubber membrane and piston friction (Bishop and Henkel, 1964; Duncan and Seed, 1967; Engineer Manual, 1970; and Gibbs et al, 1960). The magnitudes of the necessary corrections for the loads carried by rubber membrane and piston friction were calculated and their values were found to be very small compared to

the total strength of the sample; therefore, they were
neglected.

When stress is imposed upon particulate matter the
stress level is rarely large enough to cause the complete
fracture of the solid matter. Instead, failure is local-
ized, occurring between only some of the particles (Koerner
and Lord, 1972). As the stress level increases, approach-
ing the shearing resistance of the mass, failure is propa-
gated (between particles) until mass failure occurs.
When a particulate material is tested in axial compression,
the axial strain is found to be a function of breaking of
bonds and reorientation of particles due to the energy
imparted by axial stress. This was demonstrated by Pollock
(1968) and Koerner and Lord (1972) by using acoustic
emission approach (see Appendix C).

Sand-Asphalt Samples

Stress-Strain Relationships

Fig. 15 showed a typical stress-strain plot for sand-
bitumen samples tested at two different accelerations. In
this figure, the upper curve, A, corresponded to $\alpha g = 1.0g$
and lower curve, B, to $\alpha g = 1.7g$. For a particular stress
level, say $(\sigma_1 - \sigma_3) = 0.5$ Kg/cm^2, the upper curve (A)
yielded a strain of $\varepsilon = 0.32$ percent; whereas lower curve
(B) yielded strains, $\varepsilon = 0.9$ percent. This would
seem to imply that more bonds are broken and
more particles are reoriented in a system

represented by curve B than the system designated by curve A. Therefore, at the same static stress level, it would appear that higher accelerations (represented by curve B) create greater instability in the sand-asphalt system than the lower accelerations (curve A). This behavior may be explained by the higher energy transmitted to the system by accelerations.

Therefore:

$$[(\sigma_1 - \sigma_3)_{\alpha g = 1.7g}] < [(\sigma_1 - \sigma_3)_{\alpha g = 1.0g}]$$

or in general,

$$[(\sigma_1 - \sigma_3)_f \ \alpha g] < [(\sigma_1 - \sigma_3)_f \ 1.0g], \ \alpha > 1.0$$

These relations indicate that secant and tangent modulus for samples tested at higher acceleration fields (αg = 1.7g) are smaller than the samples tested at lower acceleration (αg = 1.0g).

Figure 16 showed the effect of confining pressures on the strength of bituminous aggregate samples. These results demonstrated that, for a given temperature and a given acceleration field, the tangent modulus and the deviator stress at failure increased with increasing confining pressure. Thus, the effect of confining pressure on failure strength and tangent modulus is seen to be opposite to that of acceleration. In other words, a sample subjected to higher confining pressure will exhibit greater strength. On the other hand, a sample subjected

to higher accelerations will exhibit less strength than the sample tested at 1g.

Strength Variation with Acceleration Field

1) Uniform acceleration: Test results reveal that for a given temperature level, the unconfined compressive strength decreased as accelerations increased (greater than 1g). Furthermore, each series evidenced a distinct "critical" acceleration which yielded a minimum "strength" (Figs. 17 and 18). Beyond the critical value strength increased with acceleration eventually approaching an asymptote at about 90 to 100 percent of the static unconfined strength.

The cause of strength loss with increasing acceleration (greater than 1g) is believed to be due to the breaking of adhesive bonds and the readjustment of particles. These bonds will be broken because of the higher energy transmitted to the system by accelerations greater than 1g. This has been explained in the previous section. After the critical acceleration is exceeded the higher energy due to accelerations cause the bituminous binder around the sand particles to flow out of the aggregate system. The higher the accelerations, the more flow is expected. In effect, this will reduce the amount of bitumen coating around sand particles resulting into higher point to

point contact. An increase in point to point contact
will mobilize higher frictional force as is manifest by
the strength increase recorded beyond the critical
acceleration.

Effect of Test Temperature: The physical properties
of asphalt binders are greatly dependent upon test temp-
eratures. Both viscosity and the binding strength of the
bitumen is reduced with an increase of temperature (Wood
and Goetz, 1959). Therefore, cohesive bonds between
individual particles of asphaltic mix will be more vulner-
able to increased energy of acceleration (greater than
1.0g) at higher temperatures. This was evident from Fig.
20. In this figure it was shown that the loss in strength
at higher temperatures increased as accelerations were
increased (greater than 1.0g). The lower viscosity of the
material at the higher temperatures enables the bitumen
to flow at lower induced accelerations. Therefore, the
critical accelerations decreased as the temperatures in-
creased, Fig. 21.

Effect of Confining Pressure: Oppenlander and Goetz
(1958) found that the strength of a bituminous aggregate
increased as confining pressures were increased. The
reason given for this increase in strength with confine-
ment was that the confinement mobilized higher frictional
force within the material. When an unconfined sand-
asphalt sample was subjected to increasing acceleration

fields in this study, (greater than 1g), greater strength
losses were recorded (Figs. 17 and 18). However, in con-
formity with Oppenlander and Goetz, as the confining
pressures are increased strength losses were reduced with
increasing accelerations, Figs. 19 and 20.

ii) Periodic accelerations: Test results given in
Fig. 22 revealed that for a given temperature level, the
unconfined compressive strength decreased as the magnitude
of accelerations increased (greater than 1g). The same
was true for different initial density and test tempera-
tures (Figs. 22 and 23). In these plots of periodic
acceleration, no critical acceleration was observed,
wherein there would be an increase in strength. The reason
for this behavior is that the periodic nature of accelera-
tions cause periodic fluctuations in interparticle contact
area. This would imply that there was no increase in
point to point contact as was assumed to have occurred in
samples subjected to uniform accelerations (Figs. 17, 18,
and 19). Therefore no strength increase beyond a certain
acceleration was observed.

Fig. 36 demonstrates that current standard testing
procedures based on static loadings are on the "unsafe
side". In this figure the upper curve indicates the varia-
tion in unconfined strengths under static conditions for
the mix at the indicated temperatures. The lower curve
provides the unconfined strengths at an acceleration
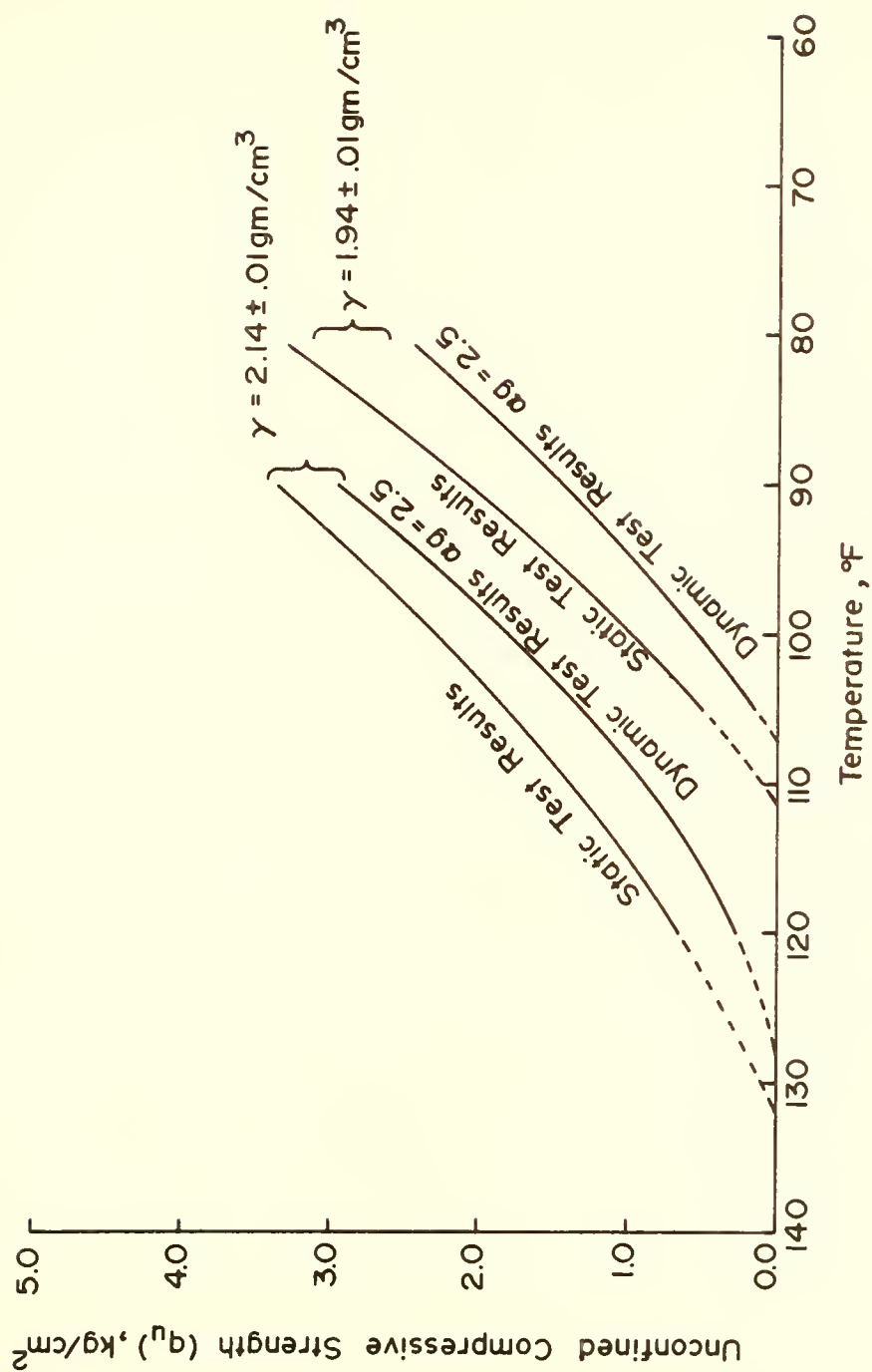
FIGURE 36 COMPARISON OF STATIC AND DYNAMIC STRENGTHS AT DIFFERENT TEMPERATURES FOR SAND-ASPHALT SAMPLES.

$\alpha g = 2.5g$. The amount of difference between static and dynamic strength will depend upon the initial density and the testing temperatures. Dynamic instability number (D.I.), which is defined as the ratio of unconfined strength at $1g$ to unconfined strength at αg, can be considered as a measure to determine the susceptibility of a mix to dynamic loads. As would be expected, Fig. 37 exhibits that a mix of low initial density subjected to high temperatures is more unstable under dynamic loads than a mix of high initial density and at a lower temperature.

Results of confined compression tests at different acceleration fields demonstrated a decrease in strength with accelerations(Figs. 24 and 25). However, both c and ϕ strength parameters were found to decrease very slightly with increasing accelerations, approaching an asymptote at $\alpha = 2.5$, Fig. 30.

In a conventional triaxial compression test the intermediate principal stress σ_2 is assumed to be equal to the minor principal stress σ_3. However, in many field situations the intermediate principal stress may be very different from the minor principal stress (Harr, 1966). The hollow cylinder testing technique was used to determine the effect of the intermediate principal stress, on the strength parameter. Results of hollow cylinder tests, conducted at two different acceleration fields, were summarized in Tables 3 and 4. Figs. 28 and 29 showed the
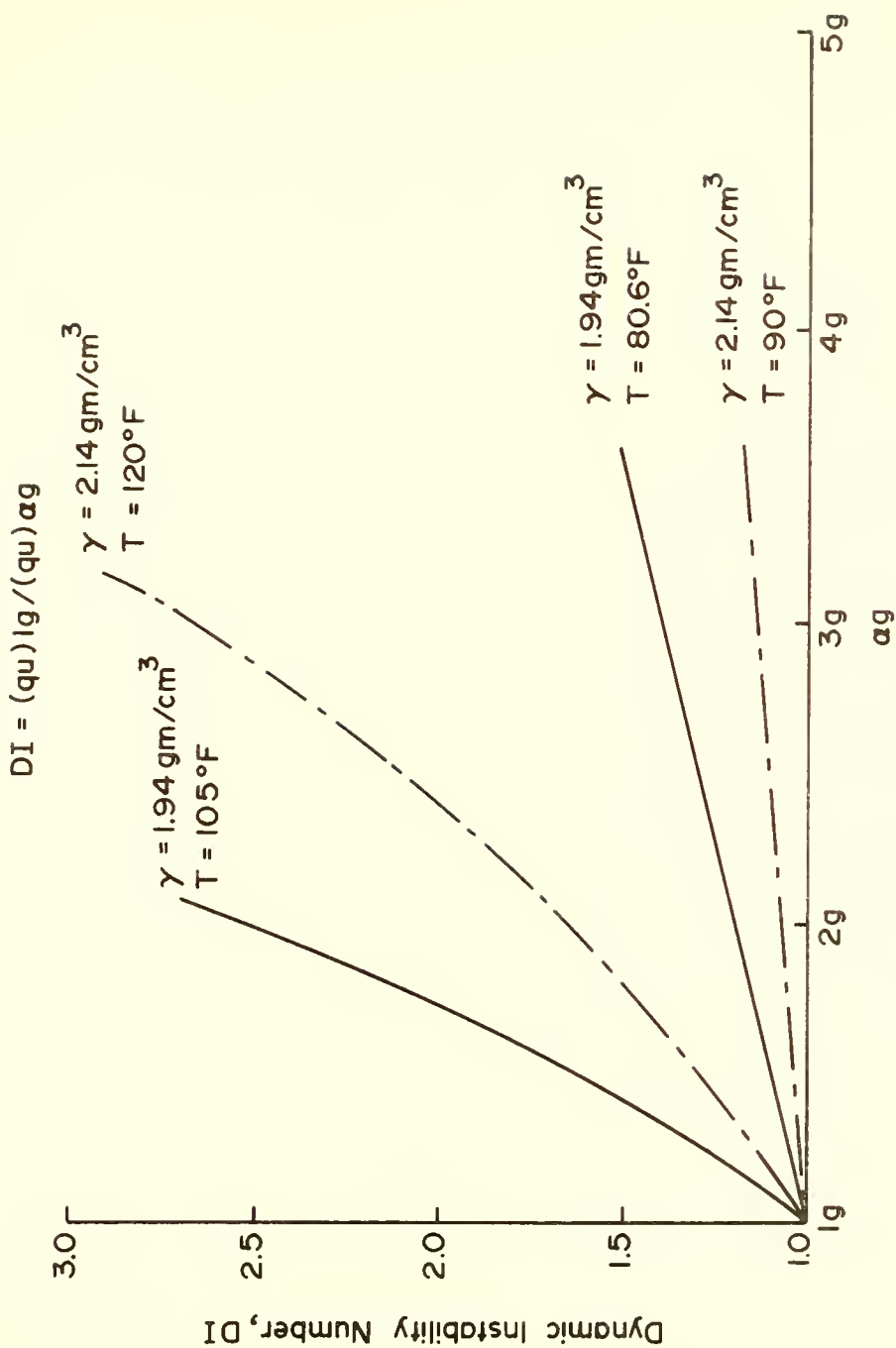
FIGURE 37 VARIATION OF DYNAMIC INSTABILITY NUMBER WITH ACCELERATION FIELDS (SAND-ASPHALT SAMPLES).

corresponding Mohr-Coulomb yield surfaces, projected on octahedral planes. The results reveal that for both accelerations, $\alpha g = 1g$ and $\alpha g = 2.5g$, hollow cylinder test results deviate but slightly from the yield surface predicted by the Mohr-Coulomb theory. Although no such test results are available in literature for asphalt samples, tests on sands show that ϕ values for hollow cylinder tests may be about 2° to 5° higher than triaxial values (Kirkpatrick, 1957; Whitman and Luscher, 1962; and Wu et al, 1963). The same tendency, of higher ϕ values for hollow cylinder tests was also observed in the present study for asphalt samples (Fig. 30); this was found to be true for acceleration fields of $\alpha = 1$ and $\alpha = 2.5$.

Cohesionless Soil

Test results reveal that for a given cohesionless soil the void ratio decreased as accelerations were increased. For a given acceleration the decrease in void ratio was greater for higher confining pressure, Fig. 31. The increased subsidence (or decrease in void ratio) with increased accelerations may be attributed to the higher energy transmitted to the system at higher acceleration fields (more than 1g). However, each level of confinement exhibited a critical acceleration beyond which there was no further densification of soil. Similar results were found by other investigators for vibratory accelerations (Barkan, 1962; Youd, 1970; and Brumund and Leonards, 1972).

Figure 32 exhibited a variation of "Relative Void Ratio" with acceleration fields. It was demonstrated that the Relative Void Ratio (R.V.R.) is independent of confining pressures and varies only with accelerations. This attribute suggests that the R.V.R. may be used to predict the settlement (ΔH) of sand deposits due to accelerations. The following relationship is recommended for this purpose (see Appendix D).

$$\Delta H = H_o \frac{(R.V.R.)}{100} \frac{e_{1g}}{(1 + e_{1g})} \tag{9}$$

where ΔH is the settlement of sand layer, H_o is the original thickness of sand layer, e_{1g} is the initial void ratio and R.V.R. is an experimental parameter obtained from a plot similar to Fig. 32.

In cohesionless soils, under static (1g) conditions, volume changes occur rapidly and generally strength increases with increasing density (Taylor, 1948). As the density of a cohesionless soil has been shown to increase with acceleration (Fig. 31), it might be expected that the shear strength of the soil should increase with increasing acceleration. Test results, presented in Fig. 33, revealed that this would indeed be the case even for increased acceleration. However, beyond a certain critical acceleration ($\alpha g = 3.0g$, in the reported case) there was no further increase in strength noted with increasing

accelerations. No marked change in density was observed beyond the critical acceleration (Fig. 31). This investigation also confirmed Johnson's (see Review of Literature earlier) observations that shear strength of cohesionless soil increases with acceleration level.

Cohesive Soil

Test results indicate that for a given compaction effort, the unconfined compressive strength decreased as accelerations were increased (Fig. 35). The strength of a compacted cohesive soil, under static conditions (1g), has been found to follow the equation (Croney et al, 1958; Aitchison, 1960; Bishop et al, 1960; and Wu, 1967):

$$\tau_{ff} = \bar{c} + [\sigma - u_a + \chi (u_a - u_w)] \tan \bar{\phi} \qquad (10)$$

The terms of this equation are explained in Appendix E. As accelerations increase, the pore pressures U_a and U_w will correspondingly increase. The increase in pore pressure occurs because of the low permeability of clay. In addition the short duration of stress increment, corresponding to the increased accelerations, will not permit the pore fluid to dissipate. An increase of pore pressure, with acceleration, will reduce the effective stress on a failure plane; consequently, a reduction of strength with increased acceleration should be and was observed (Figs. 34 and 35).

The strength loss of cohesive soils with increased accelerations reveals the fact that current standard testing procedures, which are based on static loadings, may be on the "unsafe side". If the ratio of static unconfined strength to dynamic unconfined strength (defined as dynamic instability number, D.I.) is plotted against accelerations, it is seen that the soil becomes more and more unstable as accelerations are increased, Fig. 38.

Response of Bound and Unbound Particulate Materials
Subjected to Acceleration Fields

When a particulate material is subjected to axial stress, imposed by accelerations, the energy due to acceleration is utilized in breaking of bonds (between particles) and the reorientation of the particles. In a particulate matter whose particles are bound by adhesive and/or cohesive bonds, the stress level is rarely large enough to cause the complete fracture of the whole mass. Instead, failure is localized, occurring between only some of the particles. This was the reason that accelerations did not produce any noticeable change in the density of asphaltic mix samples. The same logic applies to compacted cohesive soil samples. However, a loss in strength with increasing accelerations was recorded for these, due primarily to the localized failure between individual particles (Figs. 17, 18 and 35). On the other hand, in
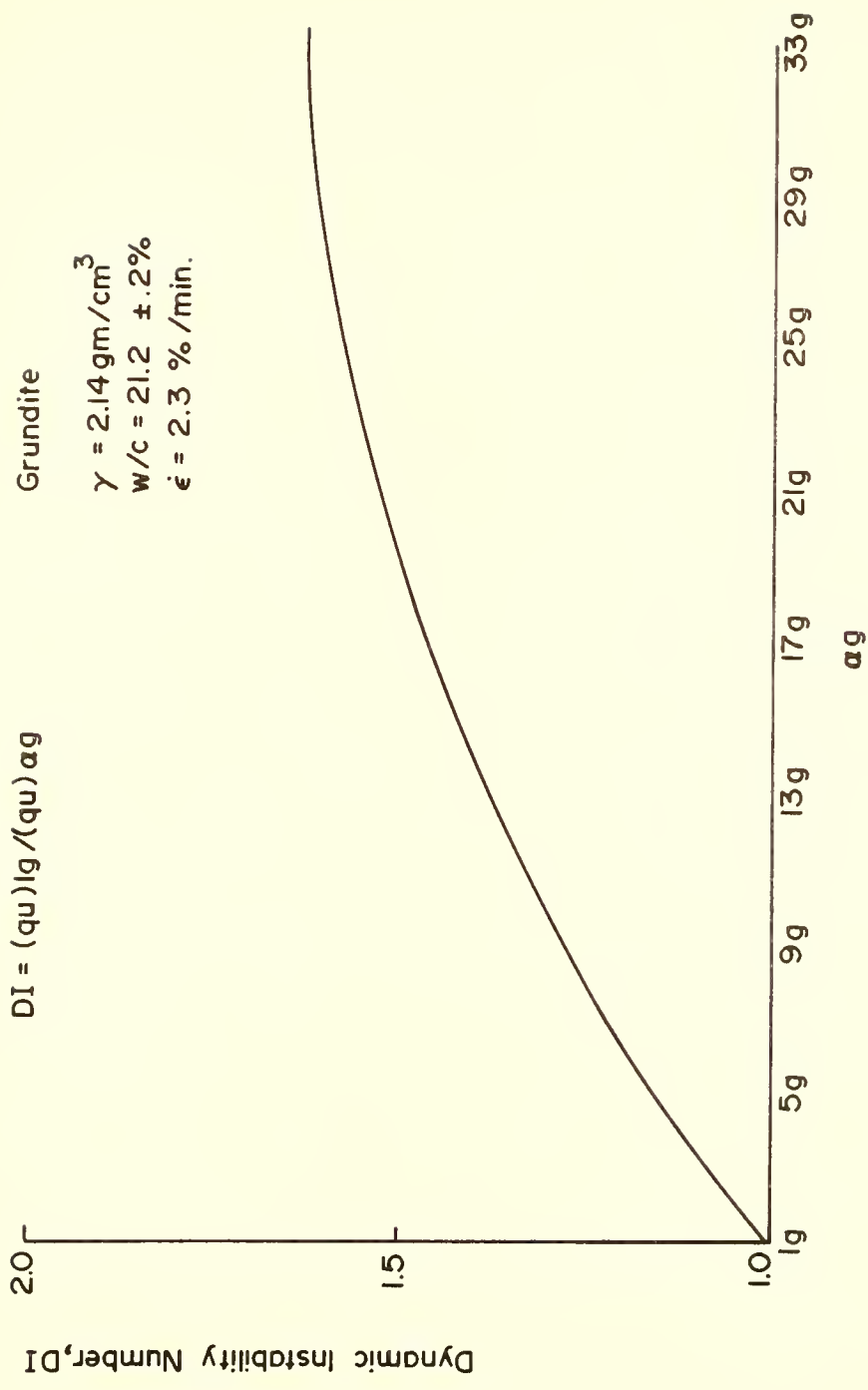
FIGURE 38 VARIATION OF DYNAMIC INSTABILITY NUMBER WITH ACCELERATION
FIELDS FOR CLAY SAMPLES.

cohesionless soils, whose particles are unbounded, the
energy imparted to the sample due to accelerations is
utilized only to readjust the particles. Consequently,
an increase in density (compaction) with acceleration was
recorded for a cohesionless soil (Fig. 31). In cohesion-
less soils strength increases with increasing density,
therefore, the shear strength of the soil increased with
increasing accelerations (Fig. 33).

SUMMARY AND CONCLUSIONS OF RESEARCH

The following conclusions have been drawn from the experimental data obtained for some common highway materials tested in this investigation.

1. A special centrifuge testing device has been designed, constructed and calibrated for this study. This apparatus models dynamic field loadings by subjecting a laboratory material specimen to different acceleration fields.

2. Triaxial compression and hollow cylinder tests on sheet-asphalt samples reveal that both strength and strength parameters decrease as accelerations greater than 1g are increased. However, the decreases in the parameters (c, ϕ) are very small. Inherent in this observation is the likelihood that strength obtained in the current standard testing procedures based on static loadings are on the unsafe side for dynamic field loadings.

3. A limited number of tests were run on dry cohesionless soil. These tests indicate that the void ratio decreases with increasing accelerations. There are indications that, for a given confining pressure, induced accelerations will increase the ultimate residual settlements.

The shear strength of the few tests on dry cohesionless soil shows only a slight initial increase with acceleration.

4. Unconfined compression tests on a compacted
cohesive soil indicate a decrease in strength as accelera-
tions are increased.

RECOMMENDATIONS FOR FURTHER RESEARCH

The following suggestions are offered for extensions of this study to improve the knowledge of basic properties of particulate materials.

1. In spite of the numbers of road tests and related research projects conducted to date, there do not exist any reliable measurements of the magnitude of accelerations experienced by highway pavements under actual traffic loadings. As such information is of paramount importance to this research, it is believed necessary that a study should be undertaken in this direction.

2. An effort should be made to measure the pore water pressure changes with acceleration in the soil samples. This measurement is necessary to understand the basic mechanism of strength variation with acceleration for soils.

BIBLIOGRAPHY

BIBLIOGRAPHY

Aitchison, G. D., "Relationships of Moisture Stress and Effective Stress Functions in Unsaturated Soils", Pore Pressure and Suction in Soil, London: Butterworth and Co. Ltd., 1960.

Avgharinos, P. J., and Schofield, A. N., "Drawdown Failures of Centrifuged Models", Proceedings of Seventh International Conference on Soil Mechanics and Foundation Engineering, Mexico City, pp. 497-505, 1969.

Barkan, D. D., Dynamics of Bases and Foundations, McGraw Hill Book Co., p. 421, 1960.

Bishop, A. W., Alpan, A., Blight, G. E., and Donald, I. B., "Factors Controlling the Strength of Partially Saturated Cohesive Soils", Proceedings American Society Civil Engineers Research Conference on Shear Strength of Cohesive Soils, p. 503, 1960.

Bishop, A. W., and Henkel, D. J., The Measurement of Soil Properties in the Triaxial Test, Edward Arnold (Publisher) Ltd., London, 1964.

Boyer , R. E., "Predicting Pavement Performance Using Time-Dependent Transfer Functions", Ph.D. Thesis, submitted to the Faculty of Purdue University, August 1972.

Brumund, W. F., and Leonards, G. A., "Subsidence of Sand Due to Surface Vibration", Journal Soil Mechanics and Foundation Division, Proceedings American Society of Civil Engineers, Vol. 98, No. SM 1, January 1972.

Bucky, P. B., "Rise of Models for the Study of Mining Problems", The American Institute of Mining and Metallurgical Engineers Technical Publication, No. 425, February, 1931.

Bucky, P. B., and Solakian, A. G., and Baldin, L. S., "Centrifugal Method of Testing Models", Civil Engineering, Vol. 5, No. 5, May 1935.

Croney, D., Coleman, J. D., and Black, W. P. M., "Movement and Distribution of Water in Soil", Highway Research Board Special Report, 40, p. 226, 1958.

Duncan, J. M., and Seed, H. B., "Corrections for Strength Test Data", Journal Soil Mechanics and Foundation Division, American Society of Civil Engineers, Vol. 93, No. SM 5, September 1967.

Engineering and Design - Laboratory Soil Testing - Engineer Manual EM 1110-2-1906, Headquarters, Department of the Army Office of the Chief Engineers, pp. X-25, November 1970.

Gau, F. L., and Olson, R. E., "Uniformity of Specimens of a Compacted Clay", Journal of Materials, JMLSA, Vol. 6, No. 4, pp. 874-888, December 1971.

Goetz, W. H., McLaughlin, J. F., and Wood, L. E., "Load-Deformation Characteristics of Bituminous Mixtures Under Various Conditions of Loadings", Proceedings of the Association of Asphalt Paving Technologists, Vol. 26, 1957.

Harr, M. E., Foundations of Theoretical Soil Mechanics, McGraw-Hill Book Company, 1966.

Highway Research Board - The AASHO Road Test - Report 6 - Special Studies, Washington, 1962.

Houwink, R., Elasticity, Plasticity and Structure of Matter, Dover Publications, Inc., 1958.

Hvorslev, M. J., "Physical Components of the Shear Strength of Saturated Clays", Proceedings American Society of Civil Engineers Research Conference on Shear Strength of Cohesive Soil, pp. 169-273, 1960.

Johnson, S. W., Smith, J. A., Franklin, E. G., Moraski, L. K., and Teal, D. J., "Gravity and Atmospheric Pressure Effects on Crater Formation in Sand", Journal of Geophysical Research, Vol. 74, No. 20, 1969.

Kirkpatrick, W. M., "The Condition of Failure of Sands", Proceedings Fourth International Conference Soil Mechanics and Foundations Engineering, Vol. 1, 1957.

Kirkpatrick, W. M., and Belshaw, D. J., "On the Interpretation of the Triaxial Test", Geotechnique, Vol. 18, No. 3, pp. 336-350, 1968.

Koerner, R. M., and Lord, A. E., "Acoustic Emissions in Medium Plasticity Clayey Silt", Journal Soil Mechanics and Foundation Division, Proceedings American Society of Civil Engineers, Vol. 98, No. SM 1, pp. 161-165, January 1972.

Lambe, T. W., and Whitman, R. V., Soil Mechanics, John Wiley and Sons, Inc., p. 234, 1969.

Lee, H. R., and Scheffel, J. L., "Runway Roughness Effects on New Aircraft Types", Journal of Aero-Space Transport Division, Proceedings American Society of Civil Engineers, November 1968.

Liptai, R. G., and Harris, D. O., "Acoustic Emission - An Introductory Review", Material Research and Standards, pp. 8-10, March 1971.

Lyndon, A., and Schofield, A. N., "Centrifuge Model Test of a Short-Term Failure in London Clay", Geotechnique, Vol. 20, No. 4, December 1970.

Mikasa, M., Takada, N., and Yamada, K., "Centrifugal Model of a Rockfill Dam", Proceedings of Seventh International Conference on Soil Mechanics and Foundation Engineering, Mexico City, 1969.

Nadai, A., Theory of Flow and Fracture of Solids, McGraw-Hill Book Company, New York, Vol. 1, 1950.

Oppenlander, J. C., and Goetz, W. H., "Triaxial Testing of Bituminous Mixtures at High Confining Pressures", Proceedings Highway Research Board, Vol. 37, December 1958.

Panek, Louis A., "Centrifugal Testing Apparatus for Mine-Structure Stress Analysis", Bureau of Mines Report of Investigations 4883, 1952.

Pokrovsky, G. I., and Fedrov, I. S., "Studies of Soil Pressure and Soil Deformations by Means of a Centrifuge", Proceedings 1st International Conference of Soil Mechanics and Foundation Engineering, Vol. 1, 1936.

Pollock, A. A., "Stress Wave Emission - A New Tool for Industry", Ultrasonics, pp. 88-92, April 1968.

Rambosek, A. J., "A Centrifuge Designed to Study Two-Dimensional Transparent Photo-Elastic Models", Bureau of Mines Report of Investigations, 1964.

Rowe, P. W., and Barden, L., "Importance of Free Ends in Triaxial Testing", Journal of the Soil Mechanics and Foundations Division, American Society of Civil Engineers, Vol. 90, No. SM 1, pp. 1-28, 1964.

Schaub, J. H., "Strength and Volume Change Characteristics of a Bituminous Mixture under Triaxial Testing", Ph.D. Thesis, submitted at Purdue University, August 1960.

Seed, H. B., and Idriss, I. M., "Simplified Procedure for Evaluating Soil Liquifaction Potential", Journal Soil Mechanics and Foundation Division, American Society of Civil Engineers, Vol. 97, No. SM 9, September 1971.

Seed, H. B., Mitchell, J. K., and Chan, C. K., "The Strength of Compacted Cohesive Soil", Proceedings American Society of Civil Engineers, Research Conference on Shear Strength of Cohesive Soil, pp. 877-964, 1960.

Seed, H. B., and Silver, M. L., "Settlement of Dry Sands During Earthquakes", Journal Soil Mechanics and Foundation Division, Proceedings American Society of Civil Engineers, Vol. 98, No. SM 4, April 1972.

Sridharan, A., "Some Studies on the Strength of Partially Saturated Clays", Ph.D. Thesis, submitted at Purdue University, August 1968.

Taylor, D. W., Fundamentals of Soil Mechanics, John Wiley and Sons, Inc., New York, pp. 347-351, 1948.

Terzaghi, K., "Simple Tests Determine Hydrostatic Uplift", Engineering News Record, p. 116, 1939.

Whitman, R. V., and Luscher, V., "Basic Experiment into Soil Structure Interaction", Journal Soil Mechanics and Foundation Division, American Society of Civil Engineers, December 1962.

Wood, L. E., "The Stress-Deformation Characteristics of Asphaltic Mixtures Under Various Conditions of Loading", Ph.D. Thesis, submitted at Purdue University, August 1956.

Wood, L. E., and Goetz, W. H., "The Relationship Between the Unconfined Compressive Strength of a Bituminous Mixture and Viscosity of the Binder", Proceedings of the Association of Asphalt Paving Technologists, Vol. 27, February 1959.

Wood, L. E., and Goetz, W. H., "The Strength of Bituminous Mixtures and Their Behavior Under Repeated Loads", Highway Research Board Proceedings, Vol. 35, March 1957.

Wu, T. H., Soil Mechanics, Allyn and Bacon, Inc., Boston, p. 81, 1967.

Wu, T. H., Loh, A. K., and Malvern, L. E., "Study of Failure Envelope of Soils", Journal Soil Mechanics and Foundation Division, American Society of Civil Engineering, February 1963.

Youd, T. L., "Densification and Shear of Sand During Vibration", Journal Soil Mechanics and Foundation Division, Proceedings American Society of Civil Engineers, Vol. 96, No. SM 3, pp. 863-880, May 1970.

APPENDICES

Appendix A

Calculation of Stresses in Hollow Cylinder

The most general form of Mohr-Coulomb failure criterion (Harr, 1966) states that

$$\sigma_{max} = \sigma_{min} \, N^2 + 2 \, CN \qquad (A-1)$$

where $N = \tan(45 + \phi/2)$.

The relationship between tangential (σ_θ) and radial (σ_r) stresses at a point inside a hollow cylinder can be written as (Harr, 1966):

$$\frac{d\sigma_r}{dr} + \frac{\sigma_r - \sigma_\theta}{r} = 0 \qquad (A-2)$$

If a test is conducted in which outside pressure (p_o) is kept constant and failure is brought by increasing the inside pressure (p_i), then equations (A-1) and (A-2) combine to give

$$\frac{d\sigma_r}{dr} + \frac{\sigma_r}{r} \left(1 - \frac{1}{N^2}\right) + \frac{2 \, CN}{N^2 r} = 0$$

Here $\sigma_r \geq \sigma_a \geq \sigma_\theta$. This can then be integrated as follows:

$$\int_{\sigma_r}^{p_o} \frac{d\sigma_r}{\sigma_r \left(-1 + \frac{1}{N^2}\right) - \frac{2 \, CN}{N^2 r}} = \int_{r}^{r_o} \frac{dr}{r}$$

to get

$$\sigma_r = \left[p_o - \frac{2\ CN}{1-N^2} \right] \left[\frac{r}{ro} \right]^{\frac{1-N^2}{N^2}} + \frac{2\ CN}{1-N^2} \tag{A-3}$$

and

$$\sigma_\theta = \left[p_o - \frac{2\ CN}{1-N^2} \right] \left[\frac{1}{N^2} \right] \left[\frac{r}{ro} \right]^{\frac{1-N^2}{N^2}} + \frac{2\ CN}{1-N^2} \tag{A-4}$$

Axial stress can be obtained by assuming uniform distribution over the horizontal section (Harr, 1966).

$$\sigma_a = \frac{p_o r_o^2 - p_i r_i^2}{r_o^2 - r_i^2} \tag{A-5}$$

where r_o and r_i are outside and inside radii and p_o and p_i are outside and inside pressures.

Appendix B

Projection Onto Octahedral Plane

Fig. B-1 shows the Mohr-Coulomb yield surface. If the principal stresses on a specimen at failure are σ_1', σ_2', and σ_3', they may be projected onto the octahedral plane $\sigma_1 + \sigma_2 + \sigma_3 = k$ where k is a constant. The projection is along the straight line 0_1BB_1. The equation of line 0_1BB_1 will be

$$\frac{(\sigma_1 - \sigma_1')}{(\sigma_1' + \psi)} = \frac{(\sigma_2 - \sigma_2')}{(\sigma_2' + \psi)} = \frac{(\sigma_3 - \sigma_3')}{(\sigma_3' + \psi)} = m \qquad (B-1)$$

The equation of plane $A_1B_2A_3B_1A_2B_3$ is

$$\sigma_1 + \sigma_2 + \sigma_3 = k \qquad (B-2)$$

Then

$$m = \frac{k - (\sigma_1' + \sigma_2' + \sigma_3')}{(\sigma_1' + \sigma_2' + \sigma_3' + \psi)} \qquad (B-3)$$

Equations (B-1) and (B-3) may be combined to yield

$$\sigma_1 = \frac{\psi(2\sigma_1' - \sigma_2' - \sigma_3') + k(\sigma_1' + \psi)}{\alpha} \qquad (B-4)$$

$$\sigma_2 = \frac{\psi(2\sigma_2' - \sigma_1' - \sigma_3') + k(\sigma_2' + \psi)}{\alpha} \qquad (B-5)$$

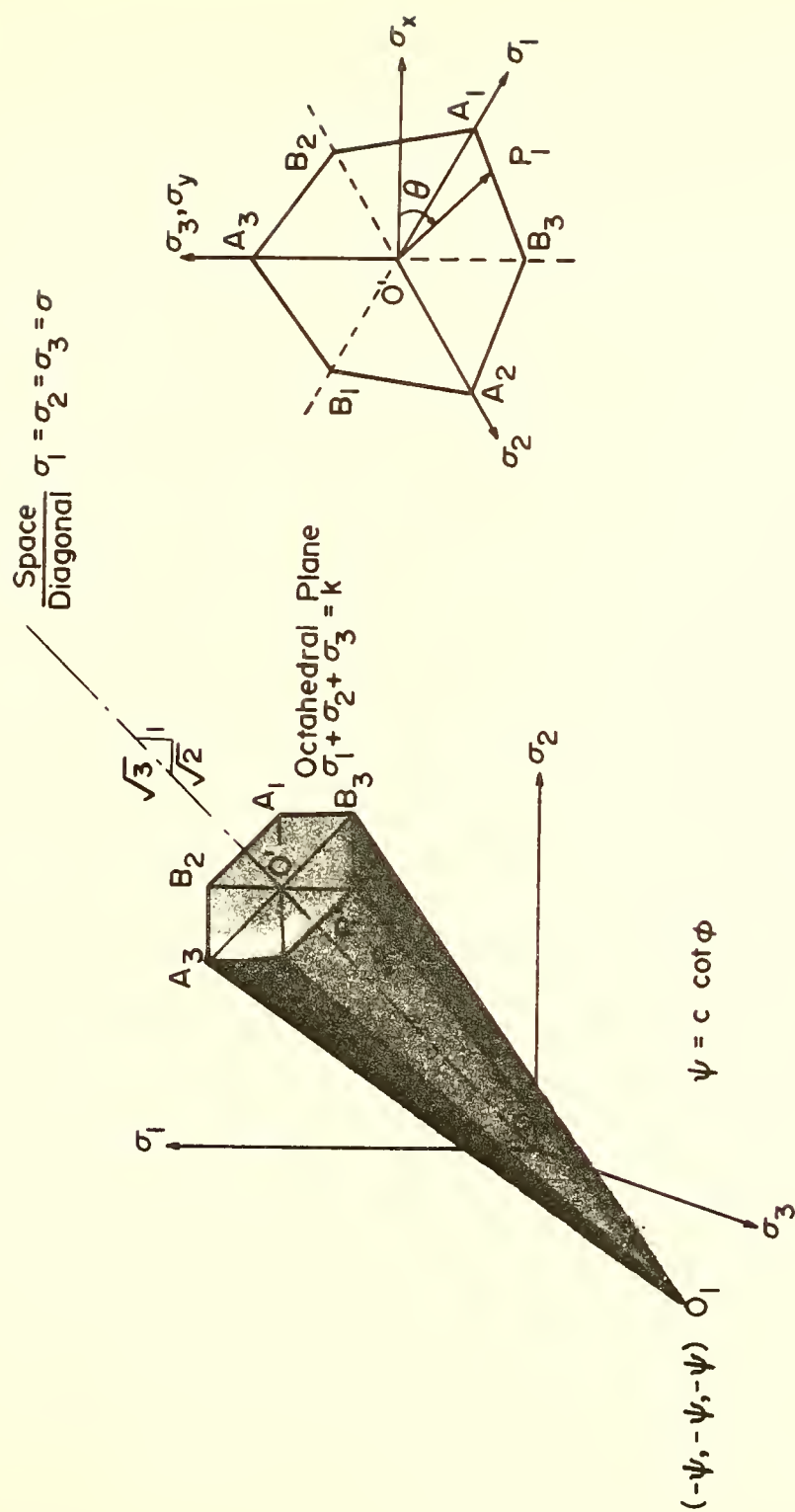$$\sigma_3 = \frac{\psi(2\sigma_3' - \sigma_2' - \sigma_1') + k(\sigma_3' + \psi)}{\alpha} \qquad (B-6)$$

FIGURE B-1 MOHR-COULOMB YIELD SURFACE AND OCTAHEDRAL PLANE .

where $\alpha = \sigma_1' + \sigma_2' + \sigma_3' + 3\psi$, and

$$\psi = C \text{ Cot } \phi$$

As the octahedral plane defines the equation $\sigma_1 + \sigma_2 + \sigma_3 = k$ and point 0, $(\sigma_1 = \sigma_2 = \sigma_3 = \sigma)$, lies on it,

$$\sigma_1 + \sigma_2 + \sigma_3 = k$$

Therefore $\sigma = k/3$. Then

$$0_1 0' = \frac{k + 3\psi}{\sqrt{3}} \qquad (B-7)$$

and

$$0_1 B_1 = \sqrt{(\sigma_1 + \psi)^2 + (\sigma_2 + \psi)^2 + (\sigma_3 + \psi)^2} \qquad (B-8)$$

Therefore,

$$B_1 0' = \sqrt{0_1 B_1^2 - 0_1 0'^2}$$

Now if the octahedral (deviatoric) plane is $A_1 B_2 A_3 B_1 A_2 B_2$ and some experimental point is P on the surface whose projection on this plane is P_1, then the coordinates of this point can be determined as shown below.

$$0' P_1 = \sqrt{0_1 P_1^2 - 0_1 0'^2}$$

$$\tan \theta = \sigma_y / \sigma_x$$

where

$$\sigma_x = \frac{\sigma_1 - \sigma_3}{\sqrt{2}}$$

and

$$\sigma_y = \frac{(\sigma_3 - \sigma_1) + (\sigma_3 - \sigma_2)}{\sqrt{6}}$$

(Harr, 1966). The terms $0'P_1$ and θ are explained in Fig. B-1, and σ_1, σ_2, σ_3 can be determined from equations (A-4), (A-5), and (A-6).

Appendix C

Acoustic Emission -

A Measure of Strength of Particulate Material

Acoustic emission approach for the measurement of strength is a fairly new approach in particulate material research. No experiments were conducted during this research to measure the acoustic emission, but the results of other investigators in this area have been used to explain the mechanism of bond breakage and reorientation of particles during stress application. Appendix C on acoustic emission has, therefore, been included here for the sake of completeness.

Acoustic emission is the term applied to the "low-level sounds" emitted by a material when it is deformed (Liptai and Harris, 1971). When the stress is imposed upon particulate matter, the stress level is rarely large enough so as to cause fracture through the solid matter, but instead failure occurs between some individual particles (Koerner and Lord, 1972). At lower stress levels failure occurs between individual particles and subaudible sounds are emitted. As the stress approaches the shearing resistance of the mass, failure is propagated between particles until mass failure occurs. Sometimes, near failure, audible noise does occur. This apparently arises from either

(i)   the breaking of adhesive bonds, and/or

(ii)   interparticle friction which is occuring

during particle reorientation and degradation.

If a particulate material, such as soil, is tested in axial compression, then the axial stress versus acoustic emission counts plot will be as shown in Fig. C-1 (Koerner and Lord, 1972). What is labeled as acoustic counts is a function of elastic energy release (Pollock, 1968), which in tern is related to strains (Koerner and Lord, 1972). Therefore, breaking of bonds and reorientation of particles is a function of axial strain.

Thus, the stress-strain curve is an indicator of breaking of bonds and reorientation of particles due to applied stress. Strength and volume changes could then be interpreted from the stress-strain relationship.
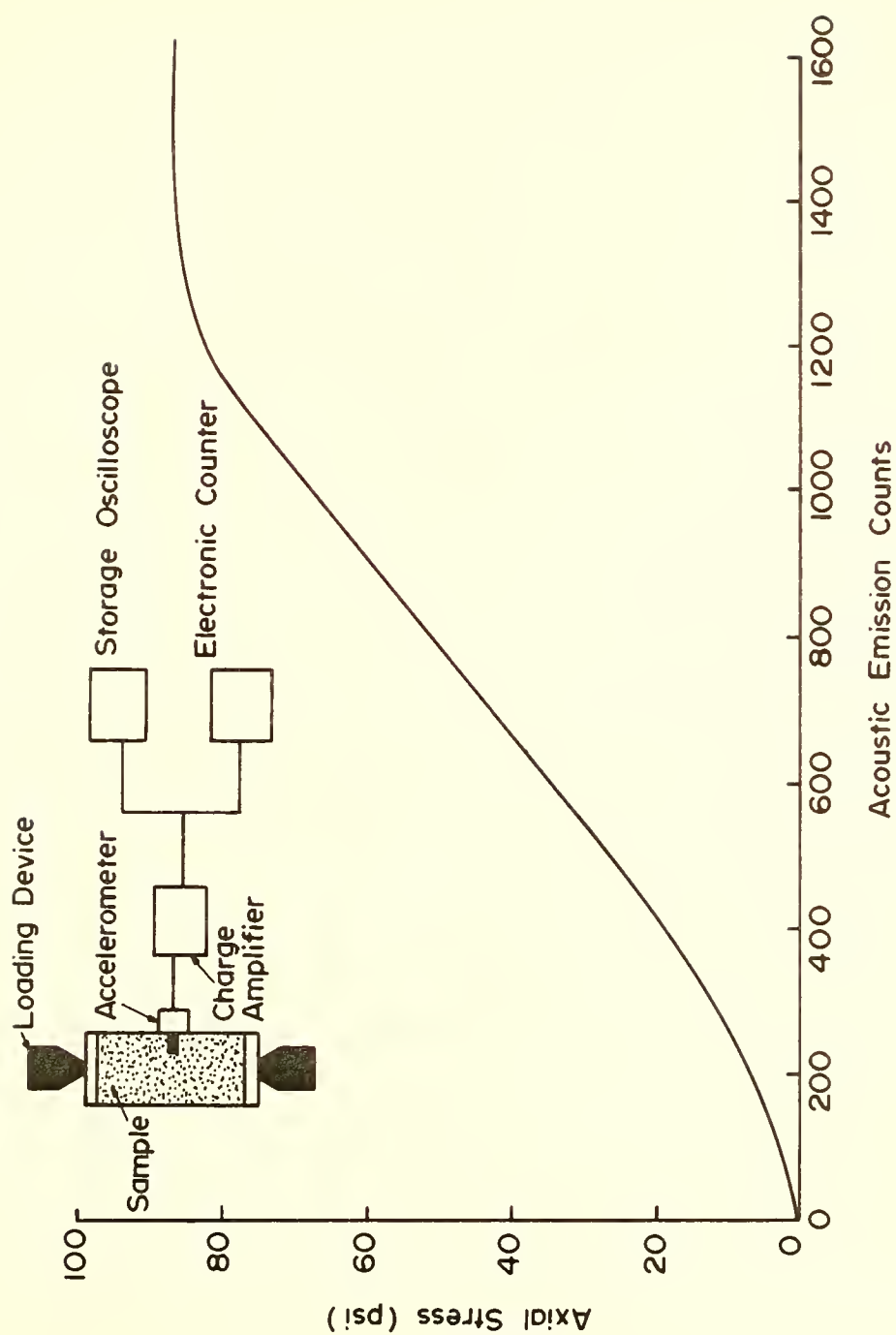
FIGURE C-I ACOUSTIC EMISSION RESPONSE OF A SOIL SAMPLE IN UNCONFINED COMPRESSION TEST (AFTER KOERNER AND LORD, 1972).

Appendix D

Settlement of Dry Sand Deposits

Due to Vertical Accelerations

The settlement of a pocket or a deposit of sand[*] due to vertical acceleration may be predicted by the formula derived below. From Fig. D-1:

$$\frac{\Delta e}{1 + e_0} = \frac{\Delta H}{H_0}$$

where H_0 is the initial height of the layer (deposit);

$e_0 = e_{1g}$ is the initial void ratio of the deposit;

ΔH is one dimensional settlement due to acceleration $= \alpha g$;

$\Delta e = e_{1g} - e_{\alpha g}$ where $e_{\alpha g} =$ void ratio at acceleration $= \alpha g$.

Therefore,

$$\frac{e_{1g} - e_{\alpha g}}{(1 + e_{1g})} = \frac{\Delta H}{H_0}$$

or

$$\Delta H = H_0 \frac{e_{1g} - e_{\alpha g}}{(1 + e_{1g})} \qquad \text{(D-1)}$$

---

[*] A dry sand deposit, when subjected to vertical accelerations (due to air blast, earthquake, etc.), may cause differential settlement of the structures (buildings or highways) supported on it. Seed and Silver (1972) have reported some case histories where settlement of dry or moist sand due to earthquakes have caused the settlement of ground surfaces with accompanying differential movements of structures.
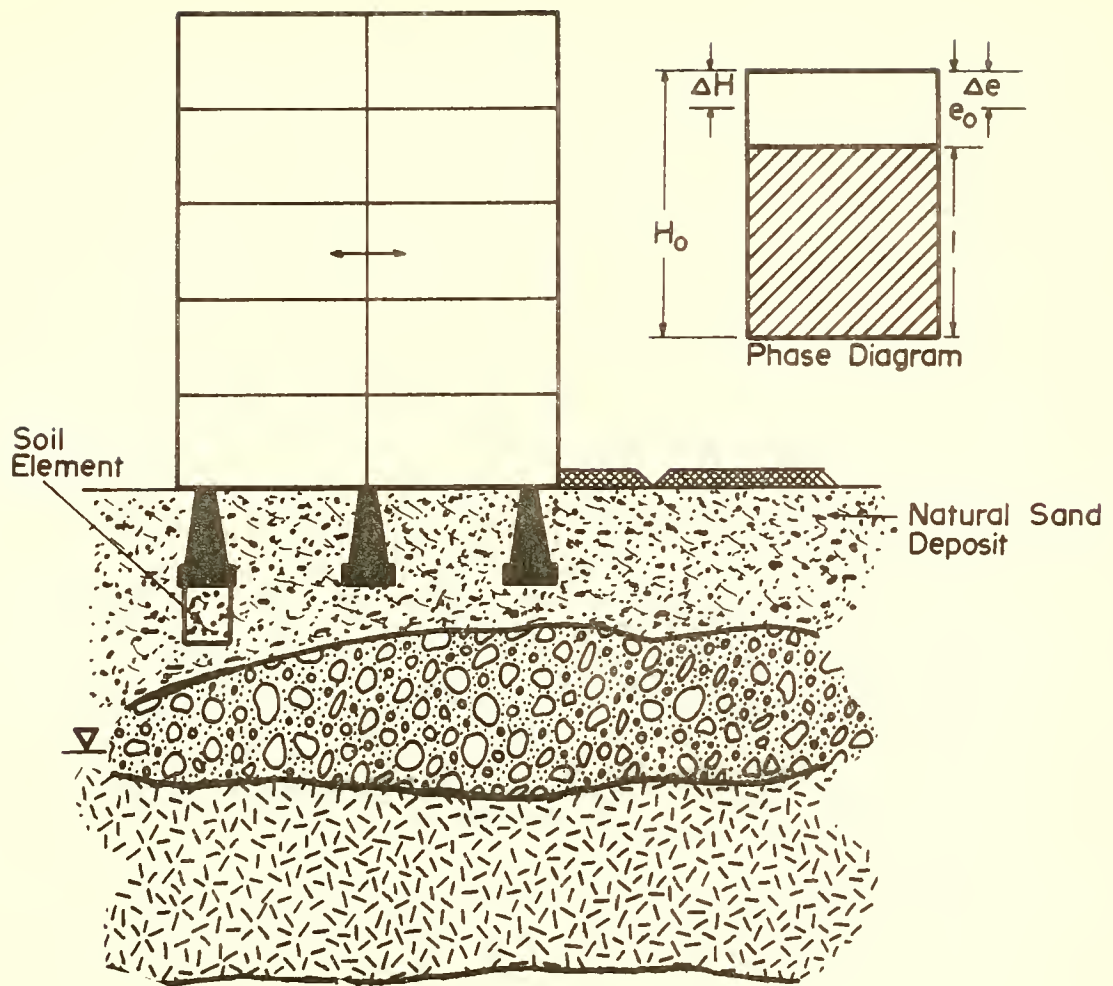
FIGURE D-I NATURAL SAND DEPOSIT SUBJECTED TO
VERTICAL ACCELERATION.

If it is defined that $\dfrac{(e_{lg} - e_{\alpha g}) 100}{e_{lg}} = R.V.R.$ (R.V.R. is

obtained from experimental results in Fig. 21), then

$$\Delta H = H_o \; \frac{(R.V.R.)}{100} \; \frac{e_{lg}}{(1 + e_{lg})} \qquad (D-2)$$

Appendix E

Effective Stresses in Three-Phase Material

Plastic flow of a particulate material can be conceived as taking place in planes which pass through the contact points between the solid particles. An idealized concept of this phenomena may be considered with respect to a sliding plane (Fig. E-1).
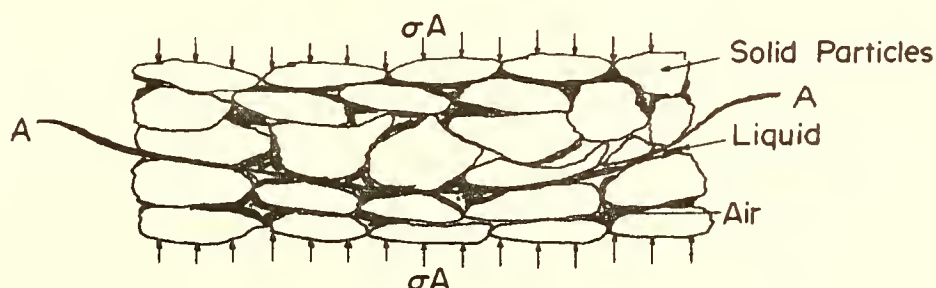

Fig. E-1   Idealized Conception of a Three-Phase Particulate Material With Regard to Plastic Flow

Across a given section AA the total force σA is composed of the following (Croney, et.al., 1958, Aitchison, 1960, Bishop, et.al., 1960, Wu, 1967).

$$\sigma A = \bar{\sigma} A + u_\ell \chi A + u_a (1-a-\chi) A \qquad (E-1)$$

where χA = the fraction of section that passes through liquid;

   u_ℓ = the pressure in liquid;

   $u_\ell = u_w$ for water

$(1-a-\chi)A$ = the fraction of section that passes through air

u_a = the air pressure

$a = \dfrac{Ac}{A}$ = the fraction of the section that is occupied by contact points.

Since the value of "a" has been shown to be very small (Terzaghi, 1939; Wu, 1967), the equation may be simplified to

$$\sigma A = \bar{\sigma}A + u_a A - \chi(u_a - u_\ell)A$$

$$\sigma = \bar{\sigma} + u_a - \chi(u_a - u_\ell)$$

$$\sigma = \bar{\sigma} + u$$

where σ = the total stress;

$\bar{\sigma}$ = the effective stress;

u = the pore pressure

$$u = u_a - \chi(u_a - u_\ell). \tag{E-2}$$

The shear strength (τ_{ff}) of the material will be expressed by the relationship

$$\tau_{ff} = \bar{c} + (\sigma - u)\tan\bar{\phi}$$

where $\bar{c}$ and $\bar{\phi}$ are the experimentally determined strength parameters.

VITA

VITA

Hari D. Sharma was born on January 4, 1943, in Utter Pradesh, India. After completing his intermediate science education from B.N.S.D. Intermediate College, Kanpur, he joined the University of Roorkee in September 1960. He received his Bachelor of Engineering degree with first division in February 1964.

Upon graduation in February 1964, Mr. Sharma joined the State Public Works Department as Assistant Engineer. In August 1964 he joined the University of Roorkee as a junior research fellow and was awarded the Master of Engineering degree with Honours in 1966.

In August 1966 he joined the staff of the University of Roorkee, India, as a Lecturer in Soil Dynamics. He resigned his position in June 1968 to join Purdue University as Graduate Assistant in Civil Engineering.

Mr. Sharma was awarded the Gold Medal for highest grades in Master of Engineering courses. He also received the Khosla Research Award for the research, "Analysis of Pile Foundations Against Earthquakes". He is a member of the Indian Society of Earthquake Technology, an associate member of the American Society of Civil Engineers and a supporting member of the Highway Research Board.

In January 1971 Mr. Sharma was married to the former Jaya Sanwal.

He is a citizen of India.